To the Graduate Council:

I am submitting herewith a dissertation written by Scott Michael Fontana entitled "Improvement of Long Range Order in Diblock Copolymer Templates for Nanostructure Deposition". I have examined the final paper copy of this dissertation for form and content and recommend that it be accepted in partial fulfillment of the requirements for the degree of Doctor of Philosophy, with a major in Chemistry.

Mark D. Dadmun, Major Professor

We have read this dissertation
and recommend its acceptance:

Accepted for the Council:

Vice Chancellor and Dean of Graduate Studies

Improvement of Long Range Order in Diblock Copolymer Templates for Nanostructure Deposition

A Dissertation

Presented for the

Doctor of Philosophy Degree

University of Tennessee, Knoxville

Scott Michael Fontana

May 2005

Thesis
2005b
.F66

Dedicated to the memory of my father,

James L. Fontana

Acknowledgements

I would first like to thank all my family whose support made this possible. I would like to especially thank my wife, Tammy for her love, support, and understanding. I would like to thank my mother, Robin, for always believing in me. I would like to thank my brother, Adam, my best friend, who has always been there for me. I would like to thank Professor Mark D. Dadmun and Dr. Douglas Lowndes for making this research possible as well as their guidance on this project and other matters. I would like to thank Charles O'Brien, Kevin Rice, Steve Wargacki, Sudesh Kamath, Asif Rasheed, Michael Lay, Nathan Crawford, Shradda Deodhar, Deepali Kumar, Rujul Mehta, Pradeep Kumar, Michael Arlen, and Eric Eastwood for their help, support, and camaraderie, each aiding to the completion of this project.

I would also like to thank Craig Hawker for his assistance with the TEMPO initiator, P.H. Flemming for her assistance in sample preparation, T.P Russell and T. Xu for their assistance on template preparation techniques, Sudesh Kamath for programming assistance, as well as A.V. Melechko and D.K. Hensley for growth of the carbon nanofibers.

This research was supported by the Office of Basic Energy Sciences, Division of Materials Sciences, US Department of Energy (DOE). Additional support was provided by the 2004 User-Initiated Nanoscience Research Program of the Center for Nanophase Materials Sciences. The research was carried out at ORNL, managed by UT-Battelle, LLC, for the US DOE under contract No. DE-AC05-00OR22725.

Abstract

This dissertation presents work that examines the use of polystyrene-*b*-poly(methyl methacrylate) (PS-*b*-PMMA) diblock copolymer thin films as nanoporous templates. Diblock copolymer thin films are able to microphase separate to produce microdomains on the nanometer length scale. Cylindrical domains can be perpendicularly oriented when cast as a thin film on a neutral surface. From the perpendicularly oriented cylindrical microdomains, nanoporous templates can be created.

Cylindrical domain block copolymer templates can lead to the production of nanostructures, but the lack of long range ordering prevents the use of diblock copolymer template for some industrial applications. Graphoepitaxy utilizes a patterned substrate to direct epitaxial growth of long range order of the cylindrical microdomains. The role of graphoepitaxial parameters including trough width and mesa height on the ordering process of cylindrical domains in diblock copolymers thin films is monitored in this study. The quantification of order was achieved by the calculation of the order parameter from the Fast Fourier transform. An increase in order was observed in samples prepared on the mesas and in troughs of widths up to 20 μm, and mesa heights in the range of 1.0 to 5.0 L_0. The role of molecular weight on the kinetics of the ordering process of cylindrical domains in diblock copolymers thin films is also examined. The kinetics of the ordering process is quantified for lower molecular weight copolymers (M_n = 63,000), but no

ordering is observed for the same time scales (up to 144 hours) for larger copolymers (M_n = 230,000). The reduction of the rate of formation of long-range order is attributed to the impeded diffusion of higher molecular weight polymers. These results demonstrate that there exists an upper limit on the molecular weights of diblock copolymers that can be used to create nanoscale templates with long range order, which also translates to an upper limit in pore size and spacing in these templates.

While diblock copolymer templates are well established as a method to produce nanoscale arrays, the size scale of the template is limited by the molecular weight of the copolymer. For larger molecular weight polymers the diffusion rate is retarded which prevents the development of long range order. This work explores the use of solvent annealing to improve long range order of high molecular weight diblock copolymer templates. By annealing copolymer thin films in a solvent rich environment increases the diffusivity of the high molecular weight copolymer increases, which improves long range order over experimental time scales.

Diblock copolymer templates are an effective method for patterning nanoscale features that are able to produce vertically aligned carbon nanofibers. We report the ability to control the size and spacing of patterned nickel nanoparticles by controlling the molecular weight of the diblock copolymer template. These nanoporous templates are able to create catalytic nickel nanoparticles with diameters as small as 18 nm with a center to center spacing of 32nm. From these catalytic nanoreactors, arrays of vertically

aligned carbon nanofibers are grown via plasma enhanced chemical vapor deposition.

Table of Contents

Chapter 1 Introduction..... 1

1.1 Diblock Copolymer Templates..... 1

1.2 Graphoepitaxial Ordering of Cylinders.....9

1.3 Solvent Annealing..... 15

1.4 Nickel Nanodots..... 19

Chapter 2 Experimental Techniques..... 25

2.1 Commercially Purchased Materials.....25

A. Chemicals..... 25

B. Polymers.....25

C. Substrates and Mask.....25

2.2 Experimental Techniques..... 26

A. Gel Permeation Chromatography..... 26

B. Nuclear Magnetic Resonance.....27

C. Spin Coating..... 28

D. Ellipsometery..... 28

E. Lithography..... 30

F. Atomic Force Microscopy..... 32

G. Fast Fourier Transform Analysis..... 35

H. Scanning Electron Microscopy & Energy Dispersive X-ray Analysis..... 37

2.3 Synthesis of Polymers.....38

2.4 Template Preparation.....41

A. Sample Preparation..... 41

B. Template Specifications.....43

2.5 Graphoepitaxy..... 43

2.6 Solvent Annealing.....44

2.7 Nickel Nano-dot Formation.....45

2.8 Carbon Nanofiber Growth.....45

Chapter 3 Long Range Order of Cylindrical Morphology Self-Assembled Diblock Copolymer Thin Films Using Graphoepitaxy..... 47

3.1 Graphoepitaxy of Cylinders..... 47

3.2 Order Parameter..... 48

3.3 Vacuum Edge..... 52

3.4 Mesa Height Effect..... 57

3.5 Trough Width..... 62

3.6 Molecular Weight..... 66

3.7 Conclusions..... 78

Chapter 4 The Use of Solvent Annealing to Improve the Kinetics of Ordering for Large Molecular Weight Diblock Copolymer Templates 79

Chapter 5 Using Self-Assembled Diblock Copolymer Thin Films to Template Nickel Nanodots for Carbon Nanofiber Growth..... 94

5.1 Nickel Deposition..... 95

5.2 Silicon Surface Neutralization..... 99

5.3 Carbon Fiber Growth..... 101

References 106

Vita 111

LIST OF FIGURES

Figure **Page**

1.1 Schematic showing the possible microdomains for a diblock copolymer as the composition is changed..... 3

1.2 Diagram of the desired orientation of the microphases that is a result of a neutral surface..... 6

1.3 Diagram depicting the removal of the PMMA cylinders by UV radiation exposure and acetic acid wash to create the nanoporous template..... 10

1.4 A). 2 μm^2 AFM image B). SEM image of the resulting nanoporous template that is created after the PMMA has been removed..... 11

1.5 Diagram depicting the patterned silicon substrate that is used for graphoepitaxially induced ordering where (W) is the width of the trough and mesa, (H) is the height of the mesa, and (X) is the thickness of the polymer film..... 12

1.6 Schematic of the solvent evaporation in a diblock copolymer film..... 18

1.7 Diagram depicting the liftoff process of a metal coated polymer template that creates an array of metal nanodots..... 22

2.1 Plot of polymer film thickness as a function of polymer concentration at 2500, from the thesis of Eric Eastwood..... 29

2.2 Schematic showing the cantilever flexes, the light from the laser is reflected onto the split photo-diode..... 34

2.3 Fast Fourier Transforms of A). Non-ordered polymer template B). Highly ordered polymer template..... 36

3.1 AFM images of 60K MW polymer prepared by spin coating. Images are 1 μm x 1 μm. A). Flat silicon substrate B). FFT image of A. C). patterned silicon substrate D). FFT image of C..... 49

3.2 FFT of an unordered polymer template and its corresponding radial and azimuthal averages..... 51

3.3 FFT of the ordered polymer template and its corresponding radial and azimuthal averages..... 53

3.4 Phase contrast image from AFM scan demonstrating the order induced by the thinning of polymer film near the mesa edge of a sample prepared from 60K molecular weight polymer on a 2.0 L_0 mesa height patterned silicon substrate that has been annealed for 18 hours at 170˚C..... 55

3.5 Height contrast AFM image along with its 3D image of demonstrating thinning of polymer film as it nears the mesa edge of a sample prepared from 60K molecular weight polymer on a 2.0 L_0 mesa height patterned silicon substrate that has been annealed for 18 hours at 170˚C..... 56

3.6 SEM image demonstrating thinning of polymer film as it nears the mesa edge of a sample prepared from 60K molecular weight polymer on a 2.0 L_0 mesa height patterned silicon substrate that has been annealed for 18 hours at 170˚C..... 58

3.7 AFM phase contrast images ~2 μm x 2 μm of varying mesa heights in 12 μm troughs prepared with 60K molecular weight polymer and annealed for 18 hours at 170 ˚C. A). 1.0 L_0, B). 1.5 L_0, C). 2.0 L_0, and D). 2.5 L_0.....59

3.8 SEM images of 60K mw polymer spin cast onto 10 L_0 mesa height patterned silicon sample and annealed at 170 ˚C for 18 hours. A). Image of the mesa that shows the order induced by polymer film thinning at vacuum edge. B). Order induced in trough only near mesa edge and lost further away from the edge..... 61

3.9 Order parameter at trough edge as a function of trough width of 60K molecular weight polymer templates prepared on patterned silicon substrate with a mesa height of 2.5 L_0 and annealed under vacuum at 170˚C for 18 hours..... 64

3.10 Ratio of the order parameter in the center of the trough divided by the order parameter at trough edge as a function of trough width of 60K molecular weight polymer templates prepared on patterned silicon substrate with a mesa height of 2.5 L_0 and annealed under vacuum at 170˚C for 18 hours..... 65

3.11 Graph depicting the evolution of the order parameter as annealing time increases for the 60K MW polymer..... 68

3.12 Graph depicting the evolution of the order parameter as annealing time increases for the 230K MW polymer.....69

3.13 Fast Fourier Transform images as annealing time increases from 1 hour to 144 hours for 60K molecular weight samples prepared on flat silicon substrate (A1, B1, and C1) compared to samples prepared on 1.5 L_0 mesa height, 16 μm wide trough, patterned silicon substrates (A2, B2, and C2)..... 71

3.14 Fast Fourier Transform images of 230K MW polymer annealed for 144 hours prepared on A. flat substrate, B. 1.5 L_0 mesa height, 16 μm wide trough, patterned substrate..... 73

4.1 Phase contrast AFM images of 230K MW diblock copolymer annealed for 96 hours..... 84

4.2 Diagram depicting the order parameter of a 230K molecular weight diblock copolymer template that has been ordered by varying techniques; Solvent annealing, Temperature annealed on flat substrates, temperature annealed on patterned substrates..... 85

4.3 Graph depicting the evolution of the order parameter as annealing time increases for the 60K MW polymer..... 89

5.1 Nickel nano-dots templated by 230 K MW polymers 70 nm thick film. A) 50 nm thick nickel. B). 75 nm C). 100 nm D). 125 nm.....97

5.2 Nickel nano-dots templated by 60 K MW polymers 32 nm thick film. A) 25 nm thick nickel. B). 40 nm C). 50 nm D). 75 nm..... 98

5.3 Nickel dots after liftoff prepared from a 60K diblock copolymer template. The template was prepared on a substrate that was neutralized via random copolymer brush..... 100

5.4 VACNF grown from 40 nm nickel dots patterned using 230K MW diblock copolymer template.....103

5.5 VACNF grown from ~18nm nickel dots patterned using a 60,000 MW diblock copolymer template..... 104

Chapter 1

INTRODUCTION

1.1 Diblock Copolymer Templates

A copolymer is a polymer chain that is composed of two or more monomers. A block copolymer is a polymer chain that is synthesized to form distinct regions, or blocks. All the monomeric units in a particular block are the same. If the polymer chain consists of two blocks with each comprised of one unique monomer, it is diblock copolymer.[1] Block copolymers can be synthesized a variety of ways. The most common method is to utilize a "living" polymerization such as anionic, or a "living" free radical polymerization.[2] "Living" polymerization allows for the synthesis of a homopolymer block that retains an active species at one end. Once the first block is synthesized to the desired chain length, the second monomer can be introduced and polymerized from the first block creating the diblock copolymer of the composition and molecular weight/chain length desired.

One feature of diblock copolymers that is of great interest above all others, is that diblock copolymers will spontaneously form microphases on the length scale of 10 to 100 nm.[2] The formation of microphases occurs because most polymers are not miscible with each other. Unlike two mixed homopolymers, diblock copolymers are covalently bound to each other. Therefore, the scale of the phase separation is limited to the size of the polymer molecules themselves.

The thermodynamics of microphase separation of a diblock copolymer can be understood as the balance of one enthalpic and two entropic contributions.[2,3] The enthalpic contribution is due to the unfavorable interaction between the two different monomers. In order to reduce the interaction between the monomers, there is a driving force to reduce their interfacial area. To this end the linkages between the blocks will be tightly packed in the minimal area, creating an interface between the blocks. To achieve this there is an entropic loss due to the fact that the blocks must to stretch into an extended chain conformation. There is also an entropic loss due to the forced localization of the block linkages at this interface.

The composition of the diblock copolymer controls the geometry of the microdomain structure.[2,3,4] As shown in Figure 1.1, a diblock copolymer will manifest a spherical microdomain when the amount of the minor phase consists of approximately 17% or less. As the amount of the minor phase is increased the microdomains will take on a cylindrical state. As the amount of the minor phase further increases a gyroid phase is formed. As the composition becomes nearly symmetrical, the diblock copolymer manifests a lamellar phase.

The molecular weight of the polymer determines the size of the microdomains. However, there are limitations to the accessible size scales of the microphase separated domains.[5] The smallest accessible domain size is limited by the product χN, where χ is the Flory-Huggins interaction parameter and N is the number of monomers in the copolymer chain,

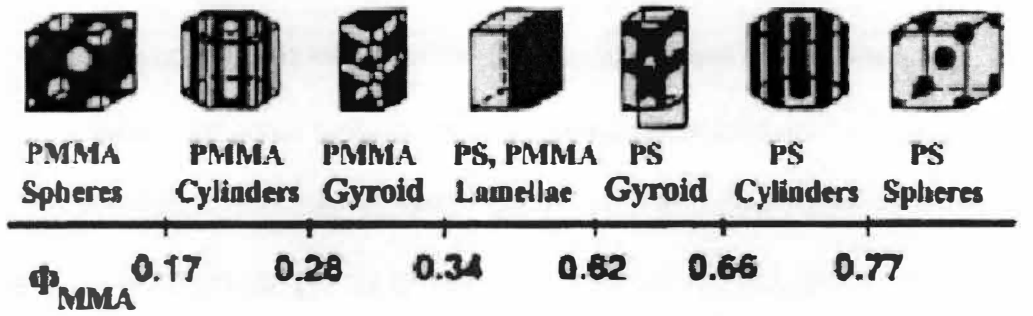

Figure 1.1: Schematic showing the possible microdomains for a diblock copolymer as the composition is changed.[2]

such that when $\chi N < 10.49$ the copolymer is phase mixed.[6] The upper size limit is set practically by the kinetics of the microphase separation process which is slow for high molecular weights.[5] The driving force for phase separation increases with molecular weight because as MW increases, N increase, thus increasing the product χN into the strong segregation regime of the phase diagram. Microphase separation occurs very rapidly in the strong segregation regime because microphase separation is a local process that requires only short-range motions of the polymer chains.

Block copolymers used in industrial applications were traditionally used as adhesives or for their mechanical properties.[3] More recently diblock copolymers have shown promise for a wide range of applications in nanotechnology. One possible application for diblock copolymers that exhibit nanoscale features is to use them to create highly ordered templates. To make full use of this technology, controlling the orientation of the microphases is imperative. In the bulk, diblock copolymers will form microdomains that have random orientations. However, controlling how the microdomains are oriented is key to utilizing diblock copolymers to pattern nanoscale features. Diblock copolymers that exhibit a cylindrical morphology hold promise to be used as nanoscale templates. To be used as templates the cylinders must be oriented perpendicular to a surface and the substrate.

Controlling surface interactions is imperative to create a perpendicular alignment of the cylindrical microdomains. Previous work by Russell has demonstrated that a diblock copolymer of poly(styrene-b-methyl

methacrylate) can be oriented perpendicular to a substrate by the control of copolymer/surface interactions.[5,7] When a diblock copolymer of PS-b-PMMA is cast onto a silicon substrate the PS will preferentially migrate to the air/polymer interface due its it's lower surface energy and the PMMA will preferentially wet the polymer/silicon interface due to hydrogen bonding interactions with the silicon oxide layer.[8] This creates a morphology in which the cylinders are oriented parallel to the silicon substrate. In order to achieve perpendicular alignment of the microdomains these preferential segregations must be over come. By creating a condition where both blocks have an equal affinity for the substrate surface, a neutral surface is creating allowing the microphases to orient perpendicularly from the substrate surface (Figure 1.2).

The neutralization of a silicon substrate can be achieved in two ways; passivating the silicon substrate, or attaching a random copolymer brush to the silicon substrate.[5,9] Passivation is achieved by removing the native silicon oxide layer with a hydrogen fluoride etch. By removing the native oxide layer, the favorable polar interactions between the PMMA and the oxide layer are eliminated. When the favorable interactions of the PMMA block to the silicon substrate are removed a condition where both blocks have an equal affinity for the substrate surface is created, thus making the surface neutral. Another method that neutralizes any favorable interactions is the utilization of a random copolymer that is end functionalized with a hydroxyl group. This functional group allows the random copolymer to bind to the silicon oxide layer on the silicon

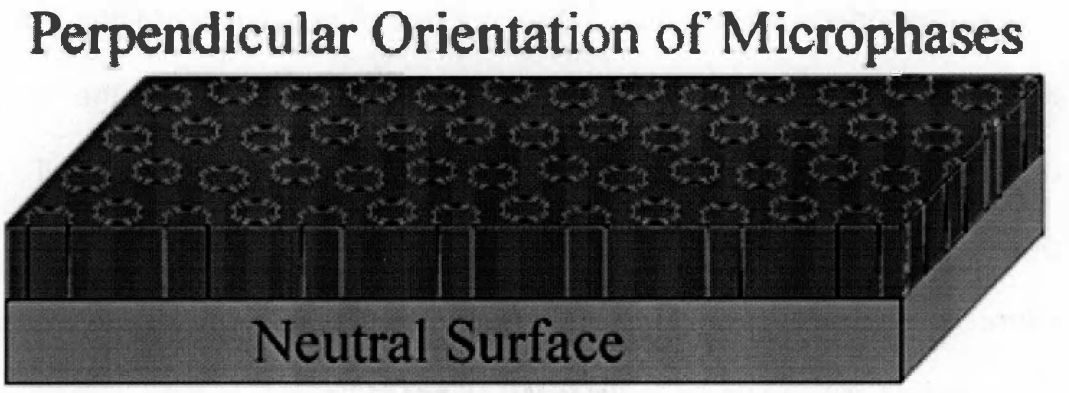

Figure 1.2: Diagram of the desired orientation of the microphases that is a result of a neutral surface.

substrate creating a brush on the silicon substrate. If the brush is to be effective in the vertical alignment process, the composition of the random copolymer must be tuned to create a neutral surface for either block. For use with a PS-b-PMMA copolymer, the random copolymer must have a mole fraction of styrene equal to 58% which was determined experimentally by Russell et. al.[9-11] Preferential segregation of either PS or PMMA to the substrate surface is prevented due to the balance of interfacial energies of the blocks with the random copolymer brush.

The preferential segregation of the PS to the air/polymer interface is due to its lower surface energy. The surface energy of PS is lower compared to the surface energy of PMMA.[12] This segregation can be eliminated by controlling the thickness of the polymer film. Kim et. al. has demonstrated that the perpendicular orientation of the domains is a function of film thickness for asymmetric diblock copolymer thin films.[13] The dependence of the orientation of cylindrical microphases on the thickness has been well studied as demonstrated in a recent review.[14] The thickness of the polymer must be equal to the center to center interdomain distance (L_0) in order to achieve the desired perpendicular orientation of the cylindrical microdomains. A polymer film of a set thickness will manifest itself in the energetically most favorable morphology of terraces with thickness equal to $(n+½)L_0$ and $(n-1/2)\ L_0$, n being any integer greater than 0, with domains parallel to the surface. [15] However, if the film thickness is ~L_0 the polymer is effectively confined to a single thickness, even if there is not confined between two hard interfaces. [16]

This is a result of the time scale of phase separation occurring much quicker than terrace formation. Therefore, with the elimination of terrace formation as an option, the film must manifest in a higher energy morphology. The lowest free energy morphology still available is a perpendicular alignment of the microdomains. [15] This reduction of free energy is sufficient to overcome the preferential segregation of PS to the air/polymer interface that is a result of the lower surface energy of PS compared to PMMA. [17] Therefore, the segregation of PS to the air/polymer interface can be overcome by the control of film thickness.

There is a sensitivity of the film thicknesses available to induce the perpendicular orientation of the microdomains. If the film thickness exceeds L_0 by a half layer or less the excess material will form islands, if the film thickness is less than L_0 by less than a half layer then the deficit is overcome by forming holes in the film.[18,19] The formation of islands and holes allows the polymer film to manifest at the correct film thickness by drawing material from adjacent areas to form terraces.

Samples that are prepared under the conditions described above and annealed above the glass transition temperature (T_g) to allow for chain mobility and reorganization, will produce an array of vertically aligned PMMA cylinders in a PS matrix. PMMA is a known negative photoresist and can be easily removed by exposing the sample to 254 nm wavelength ultraviolet light which selectively degrades PMMA by chain scission, while cross-linking

the PS matrix.[7] This is followed by a wash in acetic acid, a selective solvent for MMA, as described in previous work by Thurn-Albrecht et al.[7] (Figure1.3) The result is a nanometer scale template of hexagonally close packed pores that does not exhibit any long range ordering. (Figure 1.4)

1.2 Graphoepitaxial Ordering of Cylinders

Previous work has demonstrated that long range order of the polymer template can be improved by utilizing substrate topography to induce graphoepitaxial ordering.[20] Graphoepitaxy, or artificial epitaxy, utilizes a surface relief structure to direct epitaxial growth and improve ordering of an overlying film.[20] (Figure 1.5) Graphoepitaxy has been used for directed crystal growth of metal and polymer films.[21-23] Recently, Segalman et al. have shown that a patterned silicon substrate can induce improved long range in plane ordering of spherical domain block copolymer thin films. A copolymer of polystyrene-b-poly(2-vinylpyridine) (PS-PVP) with $f_{PVP} \sim 0.12$ was synthesized and floated onto a patterned silicon substrate. After annealing a single crystal of the diblock microphase was formed across the width of the trough.

The improved ordering is a result of the presence of a hard edge that conveys translational order onto the hexatic phase.[24] The hexatic phase is an intermediate phase of 2D melting that is between the solid and liquid phases as described by the Kosterlitz, Thouless, Halperin, Nelson, and Young theory (KTHNY theory).[25-27] The melting transition from a 2-D crystal to a liquid will proceed through an intermediate phase. This phase is the hexatic phase the

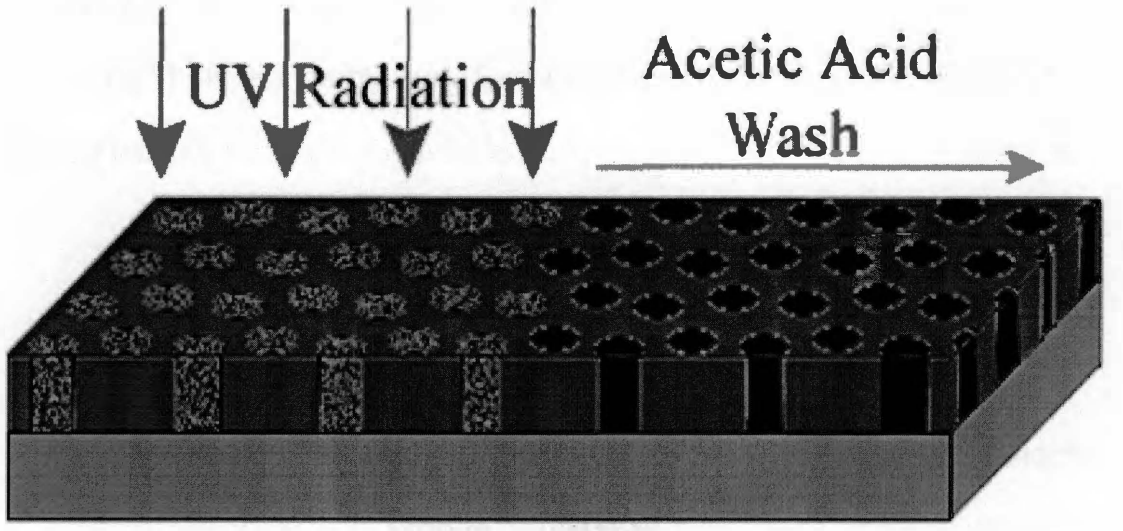

Figure 1.3: Diagram depicting the removal of the PMMA cylinders by UV radiation exposure and acetic acid wash to create the nanoporous template.

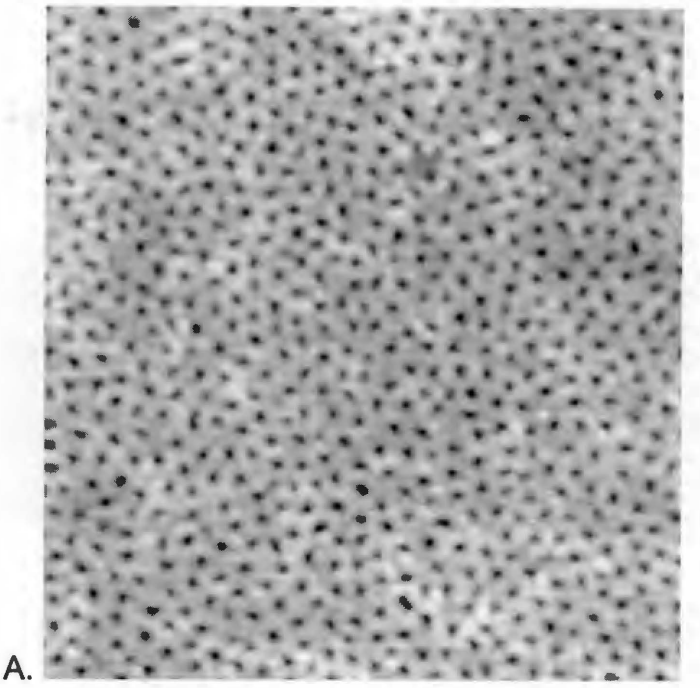

A.

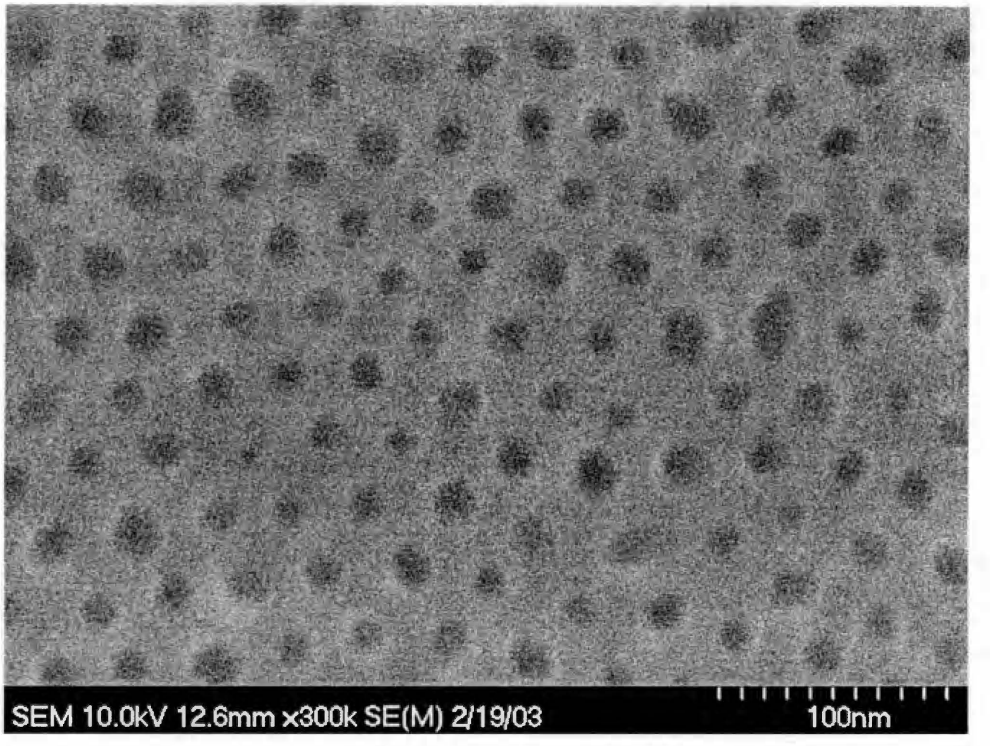

B.

Figure 1.4: A). 2 μm^2 AFM image B). SEM image of the resulting nanoporous template that is created after the PMMA has been removed.

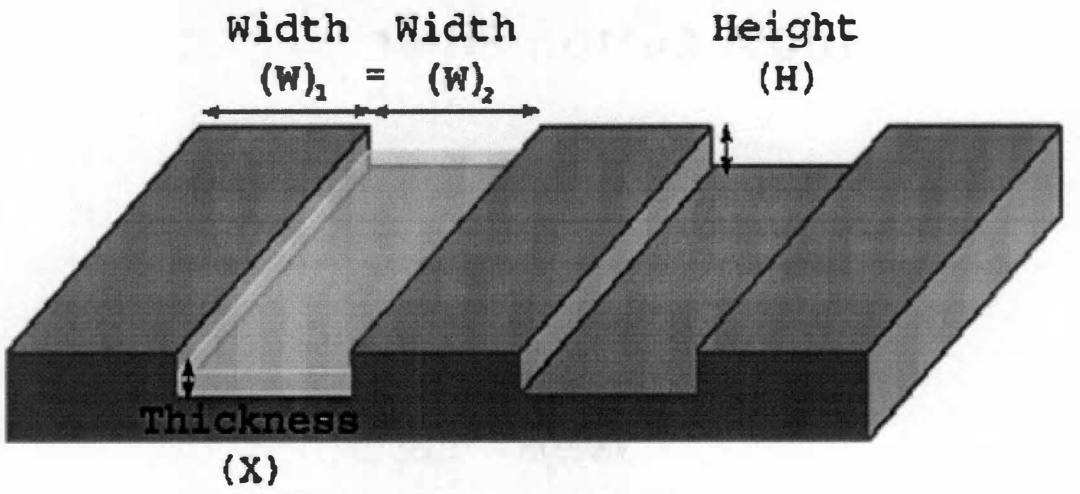

Figure 1.5: Diagram depicting the patterned silicon substrate that is used for graphoepitaxially induced ordering where (W) is the width of the trough and mesa, (H) is the height of the mesa, and (X) is the thickness of the polymer film.

which contains short-range translational order and quasi-long-range orientational order. Therefore, the molecules, or in this case the microdomains, are all oriented in the same direction relative to some fixed axis but are not separated by defined distances. Previous work has demonstrated that the edges of a patterned substrate influence the translational and orientational order in the block copolymer domains near the edge, as well as whether or not the surrounding copolymer array is polycrystalline. A consequence of this is that the 2-D hexatic to isotropic liquid transition should be a function of distance from the hard edge which has been observed in previous work.[28] This indicates that ordering that is induced at the hard edge propagates toward the center of the trough. Therefore, ordering near the edge will be equal or superior to the order that is achieved in the center of the trough.

The translational order that is achieve at the hard edge of the trough on the patterned silicon substrate is observed to be superior to the translational order that is achieved by the vacuum edge of the mesa.[24] The observations by Segalman demonstrates that the spheres are oriented in the troughs with a close packed direction that is parallel to the hard edge of the patterned substrate, which maximizes the number of spheres in close proximity to the edge. However, the spheres that are templated by the vacuum edge are a result of a different mechanism, where the polymer surface is curved at the mesa edge due to the surface energy of the polymer film. The curved polymer film thins as it approaches the edge, which

compresses the spheres closest to the edge. The curving of the polymer film near the edge reduces the surface area of the film, thus minimizing surface energy, and also reduces the thickness of the film. As there is a minimum film thickness that a single sphere can fit into, a single row of spheres is observed at a distance from the mesa edge. In the case of the cylindrical domain system, it is expected that this thinning will not induce ordering in the cylindrical morphology, as the change in film thickness should not impart the ordering of the 2-D cylinders. thereby eliminating any ordering effects the vacuum edge could have. It is not known if graphoepitaxy will be effective at inducing long range order of cylindrical morphologies of microphase separated diblock copolymers. This ordering technique been able to improve long range order in spherical domains, however cylindrical domains possess a more direct method for producing templated nanostructures.

The goal of these experiments is to understand the parameters that create the most well ordered system, not only in the troughs but on the mesas as well. A better understanding of what parameters affect the ordering process can lead to the production of highly ordered arrays of nanostructures.

Because polymer molecular weight can have such a significant effect on the kinetics of ordering, it is unknown how increasing the molecular weight of the polymer used would effect the ordering achieved by graphoepitaxy though the size of the microdomains must be affected by the molecular weight of the polymer. While currently the accessible range of microdomains size is 14 -50 nm, the ability to understand and improve the order achieved in

larger molecular weight polymers will lead to a wider range of accessible size scales from which nanostructures can be created. The ability of diblock copolymers to template nanostructures in a cost and time effective manner make them well suited for industrial applications, and if the accessible size scale is broadened a new range of applications can utilize this technology.

When the polymer is of a large enough molecular weight it may be expected that the kinetics of the system will be so severely slowed that no improvement to the ordering of the system can be observed on experimental time scales. The orientation of the microdomains occurs slowly as molecular weight increases because it requires the coordination of many chains. This coordination is limited by the rate of diffusion for the polymer chains. As molecular weight of the polymer increase the diffusivity of the molecule is reduced as shown in equation 1.1. It is not known if graphoepitaxy is an effective method for improving the long range order of high molecular weight cylindrical domain diblock copolymers.

$$D \sim N^{-2} \qquad (1.1)$$

1.3 Solvent Annealing

A more recent method that has been introduced to improve the ordering of diblock copolymer templates is the use of solvent vapor saturation of the film or solvent annealing.[29] In this technique, an improvement in ordering occurs by controlling the rate of solvent evaporation or by exposing the copolymer films to a solvent rich environment. This procedure is able to improve the long range order of the diblock copolymer template due to the

solvent swelling the polymer matrix which permits greater mobility of the polymer chains. The improved mobility of the polymer chains is a result of the solvent swelling which allows the chains to become mobile and reorganize as if they are raised above there T_g. The creation of free volume in the film is able to effectively lower the T_g of the polymer to below room temperature. The result is improved mobility of the polymer chains, which leads to the formation of highly ordered microdomains more rapidly than when the film is temperature annealed. Ordering that is achieved by this technique exhibits a strong time dependence. In recent work by Kim et al, a diblock copolymer of polystyrene-b-poly(ethylene oxide) (PS-b-PEO) was used to create a nanoporous template that was prepared using solvent annealing.[29] The removal of defects was examined as a function of exposure time. The desired ordered array is hexagonally closed packed array, therefore defects are defined as points that have either five or seven neighbors, not the desired six. This technique was able to remove half of all defects in the template within 1 hour, after 48 hours all defects had been removed from a 2 μm x 2 μm area. Unfortunately the solvent improves the mobility of the polymer chains to a level that even at room temperature the film will dewet after long anneal times.

The proposed mechanism for the induction of long range order in the polymer template is different from templates that are ordered using high

temperature annealing. The proposed mechanism ordering is initiated at the air polymer interface and diffuses down through the film.[29-32] As described earlier, copolymers that contain immiscible blocks are driven to microphase separate, the solvent mediates the non-favorable interactions between the blocks, forcing the copolymer to disorder. When the polymer film is solvent swollen the glass transition temperature (T_g) is reduced to well below room temperature due to the increase in free volume. As the solvent begins to evaporate at the polymer surface, the concentration of solvent decreases creating a solvent concentration gradient in the polymer film that is normal to the surface. (Figure 1.6) As the concentration of the solvent at the surface decreases the microphase separation of the diblock copolymer occurs only at the surface. However, the copolymer deeper in the film is still in a disordered state due to the higher level of solvent concentration. As the solvent evaporation continues the ordering propagates down through the film. While not completely understood, the formation of perpendicularly oriented cylinders is believed to be a result of the highly directional solvent gradient that is normal to the substrate. [29] Furthermore, this theory explains that the directional solvent gradient leads to the formation of cylindrical domains that are well ordered and contain high aspect ratios as determined by the film thickness.

Due to the improved kinetics of solvent annealing, this work will focus on examining the ability to use this technique to improve the long range order of perpendicularly oriented cylinders using a PS-b-PMMA diblock copolymer.

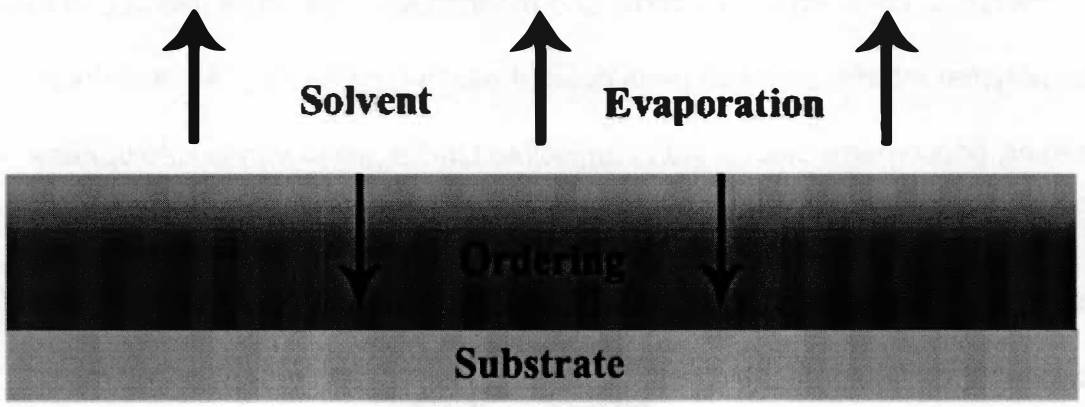

Figure 1.6: Schematic of the solvent evaporation in a diblock copolymer film. The solvent evaporates from the surface creating a solvent concentration gradient. As the solvent evaporates the ordering propagates toward the substrate producing a highly ordered oriented array of cylindrical microdomains.

The improved kinetics of solvent annealing ensures that this technique holds promise as a method to improve the long range order in high molecular weight cylindrical domain diblock copolymer templates.

1.4 Nickel Nanodots

Nanoscale arrays have numerous potential applications as field emission devices[33-35], nanoelectronics[36,37], and in nanobiotechnology. Electron beam, X-ray, and scanning tunneling microscope lithography can produce arrays of submicron dots, but are limited by low processing speed and high costs. There is also the desire to make the nanoscale arrays with smaller nanodots that are packed at higher densities, with good ordering. Electrochemical deposition is able to yield dots of 30 – 200 nanometers (nm) with controlled density, but the dot positions are random, with non-uniform size distribution. The use of a double layer of nanospheres has recently been demonstrated to produce dots as small as 30 nm.[38] In this work a self assembled monolayer of 496 nm or 1040 nm diameter PS spheres was cast onto a silicon substrate. The spheres self assembled into a hexagonally close packed array. A layer of nickel was deposited over the spheres and into the voids between the spheres. The nanospheres template was then removed by sonicating in tetrahydrofuran, a good solvent for PS, creating a pattern of nickel that was deposited through the voids of the packed PS spheres onto the silicon substrate. The resulting pattern resembles a six point star. From the nickel, a carbon nanofiber array was grown.

Polymer templates have been used to create nanoscale arrays of hexagonally ordered metal dots. Park et al has shown a method to create these arrays by utilizing block copolymer self-assembly and a trilayer pattern transfer technique.[39] Their worked utilized polyisoprene (PI) spheres in a polystyrene (PS) matrix to pattern a layer of silicon nitride by reactive ion etching (RIE). The trilayer arrangement consists of a monolayer of PI spheres in a PS matrix that is cast onto a silicon nitride layer which was prepared over a polyimide layer based on a silicon substrate. The sample is exposed to ozone which degrades the PI spheres, leaving voids. The sample is then exposed to a RIE which etches down through the polymer layer and is accelerated in the regions where the voids are present. This pattern is transferred to an underlying layer of polyimide by continuing the RIE. Ti/Au nanodots are subsequently produced by evaporating metals onto the template then lifting off the polyimide template, leaving behind a hexagonally ordered array of metal dots.

Shin presented a more direct method to produce an array of metal dots utilizing block copolymer templates with cylindrical microdomains.[40] Using this method eliminates the need for RIE which improves the fidelity with which the pattern can be replicated. This method utilizes a diblock copolymer template of PS-b-PMMA with cylindrical microdomains in which the minor PMMA phase has been removed. A thin layer of chromium was evaporated onto the surface, covering the template and partially filling the pores. The polymer template was then lifted off using sonication in toluene, followed by a

short oxygen RIE to remove any remaining polymer, leaving only a hexagonally ordered array of metal dots.

The use of microphase separated diblock copolymer templates can provide a size range of 14 – 50 nm, with interdomain spacing (L_0) as low as 30 nm.[5] No other technique has to ability to pattern such small features in close proximity while maintaining a cost effectiveness and process simplicity that far exceeds any other. Thus it will be interesting to examine templates that can be produced utilizing microphase separated diblock copolymers to be used for patterning nanometer scale reactors. An array of nanoreactors is produced by depositing catalytic nickel into the pores of the template. This can be achieved by the method set forth by Shin et al.[40] A layer of nickel is deposited over the polymer template which coats the polymer matrix as well as the substrate at the bottom of the pores. (Figure 1.7) The polymer template can then be chemically removed leaving an array of nickel nanodots. By utilizing the diblock copolymer template.method, control over the pattern, size and spacing of the dots that are produced can be obtained.

In this work arrays of catalytic nickel nanodots will be produced. From these arrays of nickel dots vertically aligned carbon nanofibers (VACNFs) will be produced using plasma-enhanced chemical vapor deposition. (PECVD) [41,42] The are two different CNF growth modes, tip-type or base-type. The growth mode depends on the ratio of acetylene, the carbon supply, to ammonia gas, etchant, flow concentration. Tip-type CNFs are vertically

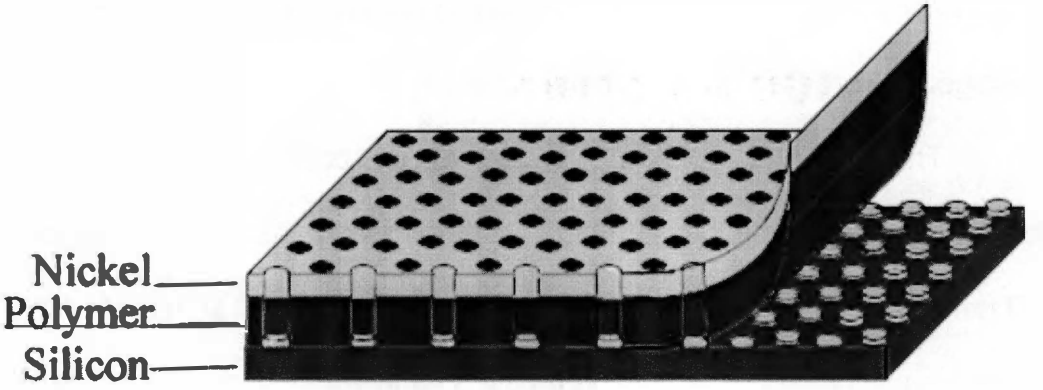

Figure 1.7: Diagram depicting the liftoff process of a metal coated polymer template that creates an array of metal nanodots

aligned, while the base-type are not. The alignment is due to the interaction between the strong electric field at the substrate and the location of the carbon precipitation at the bas of the nanoparticle which is on the tip of the nanofiber. This work is only concerned with the tip-type growth process due to its vertical alignment. During the tip-type CVD growth process carbon diffuses into the catalytic nickel particle from all directions and a carbon shell is formed at the catalyst-substrate interface. This shell limits further diffusion of carbon at the catalyst-substrate interface, which creates a concentration gradient within the catalytic nanoparticle with very few carbon atoms at the interface with the carbon shell and many diffusing carbon atoms at the interface with no carbon shell. This concentration gradient directs the carbon flow through the catalyst particle and the fiber grows.[43] These carbon fibers are not composed of single grains and are therefore properly called vertically aligned carbon nanofibers (VACNFs) not carbon nanotubes which are structurally near perfect. VACNFs have multiple crystal grains that are small compared to its circumference, while a CNT is a perfect single crystal.[42] Individual CNFs will grow only if the catalytic nickel dot is below the critical size which has been experimentally determined to be 350 nm, above this size multiple VACNFs are formed from a single dot.[42]

In this work we will examine the use of polymer templates to control the pattern, size and spacing of the VACNFs that are produced. This will be achieved by applying the tunable domain size of microphase separated

diblock copolymers to produce arrays of catalytic nickel dots of controlled diameter and spacing.

Chapter 2

EXPERIMENTAL TECHNIQUES

2.1 Commercially Purchased Materials

A. Chemicals

Styrene and methyl methacrylate monomers used for polymer synthesis were purchased from Sigma-Aldrich Chemical Company and were used as received. The solvents toluene, acetone, methanol, acetic acid, hydrofluoric acid and tetrahydrofuran used during the polymer synthesis and template preparation procedures were purchased from Fisher Scientific and used as received. Initiator and catalytic chemicals for polymer synthesis consisting of p-Toluenesulfonyl Chloride and Copper (I) Chloride were purchased from Acros Chemicals and used as received. The co-catalyst 2,2'-Dipyridyl was purchased from Sigma-Aldrich and used as received

B. Polymers

The diblock copolymer polystyrene-b-methyl methacrylate (PS-b-PMMA) (M_n = 230,700, PDI = 1.19, f_{pmma}=0.29) was purchased from Polymer Source, Inc. and was used as received.

C. Substrates and Mask

Four inch diameter silicon wafers with <100> crystal orientation, thickness of 450 – 575 μm, and N doped were purchased from International Wafer Service Inc. Portola Valley, CA. No additional treatment was performed

before their use. The large wafers were cut into smaller samples using a diamond tipped etching pen.

The photolithography mask used for patterning the silicon substrates for the graphoepitaxy study was custom made by Advance Reproductions Corporation North Andover, MA. The mask is soda-lime glass with a chrome pattern as shown in Figure 1.5

2.2 Experimental Techniques

A. Gel Permeation Chromatography (GPC)

Gel permeation chromatography (GPC) is the method used to determine the molecular weight of the polymers synthesized for these experiments. In this technique the polymer sample is separated by size using a column of porous material. In order to determine the actual molecular weight of the sample, well-characterized, narrow molecular weight standard samples must be ran through the GPC column to calibrate the instrument. Molecular weight and molecular weight distributions of an unknown sample can be ascertained by correlating elution times of the standard with those of the unknown.

The polymers for this study were characterized by a Polymer Labs gel permeation chromatograph (GPC) equipped with 2 Polymer Labs PLgel 5μm mixed-C columns with HPLC grade tetrahydrofuran as the elutant. The instrument utilized a refractive index detector to detect the polymer in solution. Samples were prepared by dissolving the polymer in tetrahydrofuran with a concentration of 2 mg/ml. Results were analyzed using

narrow molecular weight polystyrene standards for the calibration of the instrument.

B. Nuclear Magnetic Resonance Spectroscopy (NMR)

Nuclear magnetic resonance spectroscopy (NMR) is used in this work to determine the composition for polymers. Analysis was performed on a Bruker 300 MHz NMR. Samples were prepared by dissolving a small amount of polymer in d-chloroform in a NMR tube.

The composition of PS-PMMA copolymers, both random and blocky, can be determined by comparing the area under the aromatic peaks (A) to the area of non-aromatic (N). For PS-PMMA copolymer there are 5 aromatic hydrogens and 3 non-aromatic hydrogens from the styrene, while there are 8 non-aromatic hydrogens in the PMMA. The area under of the peak of the aromatic region (6.0 – 7.5 ppm) is divided by 5 to give (A). Three is subtracted from the integral of the peak area from the non-aromatic region (0.5 – 3.5 ppm) to remove the contribution of the 3 non-aromatic styrene hydrogens. This number is then divided by 8 because PMMA contains 8 non-aromatic hydrogens resulting in a normalized value for PMMA content (N). The normalized PMMA content (N) is divided by the total PS and PMMA content (sum of A and N) and multiplied by 100 giving the percent PMMA content in the polymer as seen in equation 2.1.

$$N / (A + N) \times 100 = \%PMMA \qquad (2.1)$$

C. Spin Coating

A Headway Research Inc. (model PWM32) spin coater was used to create the thin polymer films needed for this research. Rotation speed along with solution concentration can be varied to achieve desired film thicknesses with great resolution and reproducibility. In spin coating, the substrate is placed on a vacuum chuck and a solution consisting of the desired sample concentration in an appropriate solvent is deposited onto the substrate by coving the entire sample with the solution, which is then spun at the desired speed for a determined length of time. During the acceleration and spinning, all the solvent evaporates leaving a thin polymer film. The resulting polymer film thickness is a function of solution concentration, chuck speed, and solvent volatility.

Polymer solutions consisting of the desired polymer and toluene were made and then filtered and coated onto the modified silicon substrates as described in section 2.4. Film thicknesses were tuned using ellipsometery to determine appropriate spin speed and solution concentration to achieve the desired film thicknesses. A plot of polymer concentration as a function of polymer thickness at a spin speed of 2500 rpm is given in Figure 2.1. Reproducibility within 2 nm was desired and achieved.

D. Ellipsometery

This nondestructive technique is used to determine the thickness of a sample if its refractive index is known. Ellipsometry measures the change in

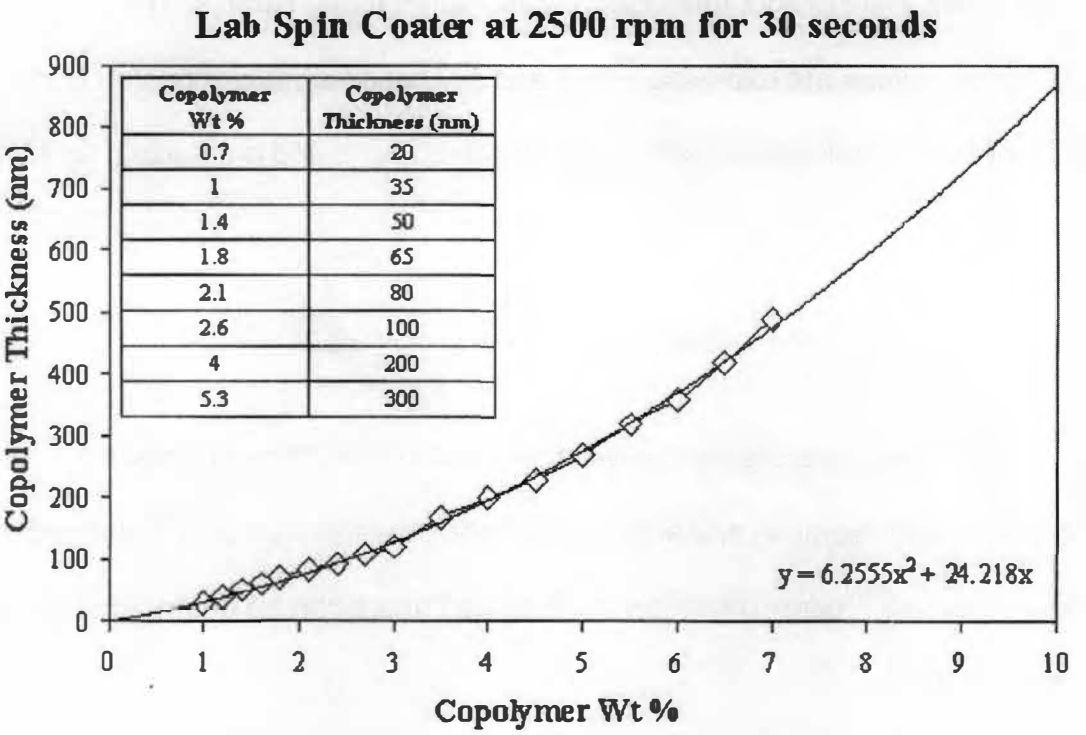

Figure 2.1: Plot of polymer film thickness as a function of polymer concentration at 2500. From the thesis by Eric Eastwood. [44]

polarization state of light reflected from the surface of a sample. The measured values are expressed as Ψ and Δ. These values are related to the ratio of Fresnel reflection coefficients, R_p and R_s for *p* and *s*-polarized light, respectively. [45]

$$\tan(\Psi)e^{i\Delta} = \frac{R_p}{R_s} \qquad (2.2)$$

P-polarized light and *s*-polarized will be reflected with different Fresnel reflection coefficients in any angle of incidence greater than 0° and less than 90°. From the Fresnel reflection coefficients $\Psi$and Δ can be determined using equation 2.2

In this work polymer samples on silicon substrate were analyzed by a DRE-Dr. Riss Ellipsometerbau GmbH (model EL X-02C) ellipsometer. A class IIIA laser at 632.8nm was used for the incident radiation and a 70˚ angle was maintained for all measurements. Silicon oxide measurements were taken with the refractive index set a 1.46 and polymer samples assumed a uniform refractive index of 1.6 because the major phase (PS) has a refractive index of 1.6, while PMMA has a refractive index of 1.5.

E. Lithography

Lithography is the process of transferring a pattern from a mask to substrate. Two types of lithography were employed in this work to prepare silicon substrates for graphoepitaxial ordering; photolithography and plasma etching. The first step in the process is photolithography. In photolithography a pattern is transferred from a mask to a polymer photoresist spin cast onto

the silicon substrate. The wafer must first be primed by cleaning with a solvent, usually Hexamethyldisilazane (HMDS), which will remove any moisture and any foreign objects such as dust.[46] The photoresist is then spin cast onto the wafer. A photoresist is a polymer substance that changes its chemical reactivity characteristics when it is exposed to certain wavelengths of light.[46] In this work a positive photoresist is used. Positive photoresists become softened when they are exposed to the correct wavelength of light. The softened areas are then removed during the chemical developing process that uses a solvent to selectively dissolve the softened areas. The desired pattern is transferred to the photoresist by using a mask. The mask consists of the desired pattern constructed from material that is either transparent or opaque to ultra violet (UV) light. The mask can then be used in the contact printing technique which places the resist coated wafer in physical contact with the mask. The resist is exposed to the beam of UV light through the mask for a fixed amount of time.[47] After exposure the wafer is placed in a developing solution to remove the exposed photoresist leaving a pattern in the photoresist.

In order to transfer the pattern from the photoresist to silicon wafer plasma etching or dry etching is employed. The dry etching technique uses plasma is to etch into the substrate. The major benefit of plasma etching verse wet chemical etch techniques is the elimination of undercutting. Wet chemical etching techniques can lead to lateral etching under the mask.[48] Plasma is a partially ionized gas composed of electrons, ions, and neutral

species that is formed by applying a large electric or magnetic field to a volume of gas. Similar to photolithography a mask is required to produce a pattern in the silicon substrate. Following the photolithography procedure the silicon wafer has photoresist on the surface that is patterned from the mask. The photoresist is not a good mask for the plasma etching procedure because the rate of photoresist removal is similar to the rate of silicon removal. To correct for this problem, the photoresist is coated with a 20 nm thick layer of chromium (Cr) as this metal is a good mask for the CF_4 plasma silicon etch. After the entire wafer is coated with Cr it is sonicated in acetone, a good solvent for the photoresist, which removes the photoresist and the overlaying Cr leaving a negative of the original pattern. The wafer is then exposed to the CF_4 plasma for a controlled amount of time where the etch depth is dependant on the exposure time. The etching of silicon by CF_4 is a well understood process which results in the gasification of silicon to form SiF_2 and SiF_4 as the dominant products.[48] Following the plasma etch, the Cr mask must be removed, which is accomplished by a wet etch technique using a chromium etchant purchased from Transene company.

F. Atomic Force Microscopy (AFM)

Ordering of the pores was determined by examination with a Digital Instruments Dimension 3500 scanning force microscope in tapping mode. Images were collected in height contrast and phase contrast modes. Atomic force microscopes measure topography with a force probe. To acquire an image the microscope raster scans the probe over the sample surface. The

probe is a tip on the end of a cantilever which bends in response to forces between the tip and the sample. As the cantilever flexes, the light from the laser is reflected onto a split photo-diode. (Figure 2.2) Vertical resolution of <1 angstrom and lateral resolution of 10 angstrom can be achieved, but vertical resolution as good as 10 pm has been reported.[49] Since AFM is a scanned probe system it does not use lenses, so the size of the probe rather than diffraction effects generally limits the resolution achieved. Because the cantilever-to-detector distance is thousands of times the length of the cantilever, the optical lever greatly magnifies motions of the tip allowing for great resolution. Images were collected in height and phase contrast using tapping mode. When the instrument is in tapping mode the cantilever is positioned above the surface and oscillated so that it only taps the surface for a very small fraction of its oscillation period. In tapping mode the lateral forces exhibited on the tip are dramatically reduced compared to the forces encountered when in contact mode. Therefore, tapping mode is ideal for imaging soft samples such as polymers.

Samples to be examined by AFM require no special preparations. Since all the samples for this work that were examined by AFM were polymer films cast on silicon substrates they were readily imaged. Data collected from the instrument was analyzed using WSxM, a freeware AFM analysis program. This program provided a method for image resizing, zooming, and fast Fourier transform analysis.

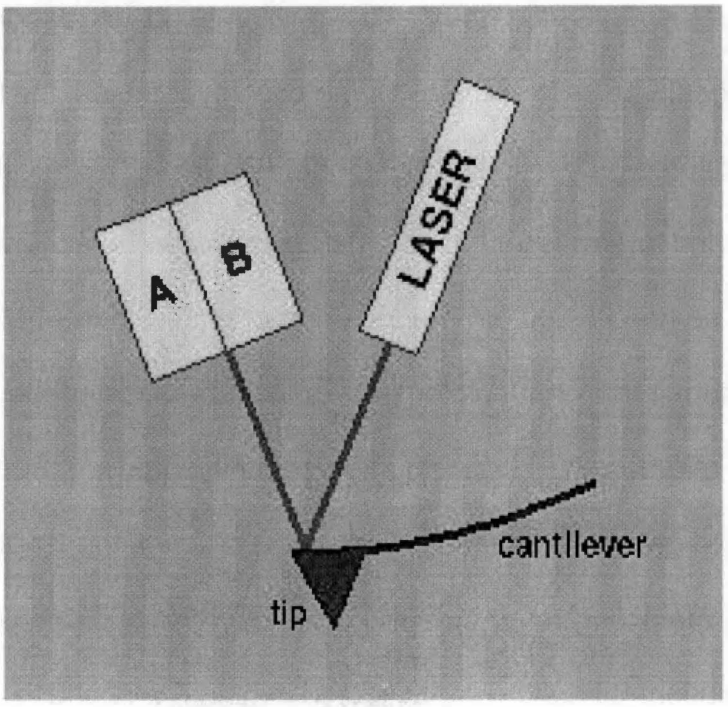

Figure 2.2: Schematic showing the cantilever flexes, the light from the laser is reflected onto the split photo-diode. [50]

G. Fast Fourier Transform Analysis

In order to effectively analyze the improvement in ordering that is achieved by using graphoepitaxy, computer analysis of the template is used. The fast Fourier transform analysis of the AFM images of the template provides a view of how well ordered the polymer templates are. Fast Fourier transforms provide a mathematical analysis of the image that is similar to producing a diffraction pattern. From this "diffraction pattern" information on the order in the system can be obtained. Figure 2.3A is a FFT of a non ordered polymer template. The doughnut shape of the FFT represents only local ordering, where all the cylinders are a fixed distance apart but are oriented randomly. Figure 2.3B, represents a more well-ordered system where the cylinders are all a fixed distance apart, and are positioned at exact points relative to each other. However, a more quantitative method for describing the order is needed to quantify the effectiveness of graphoepitaxy to induce long range order in the diblock copolymer thin film templates.

Calculating an ordering parameter from the FFT provides a quantitative measure of the order present in the polymer template. An order parameter is often used when looking at crystalline structures, or alignment of molecules.[51] The order parameter is calculated by comparing experimental results with a model of a perfect system. A completely unordered system has an order parameter of 0 while a perfectly ordered system has an order parameter equal to 1.

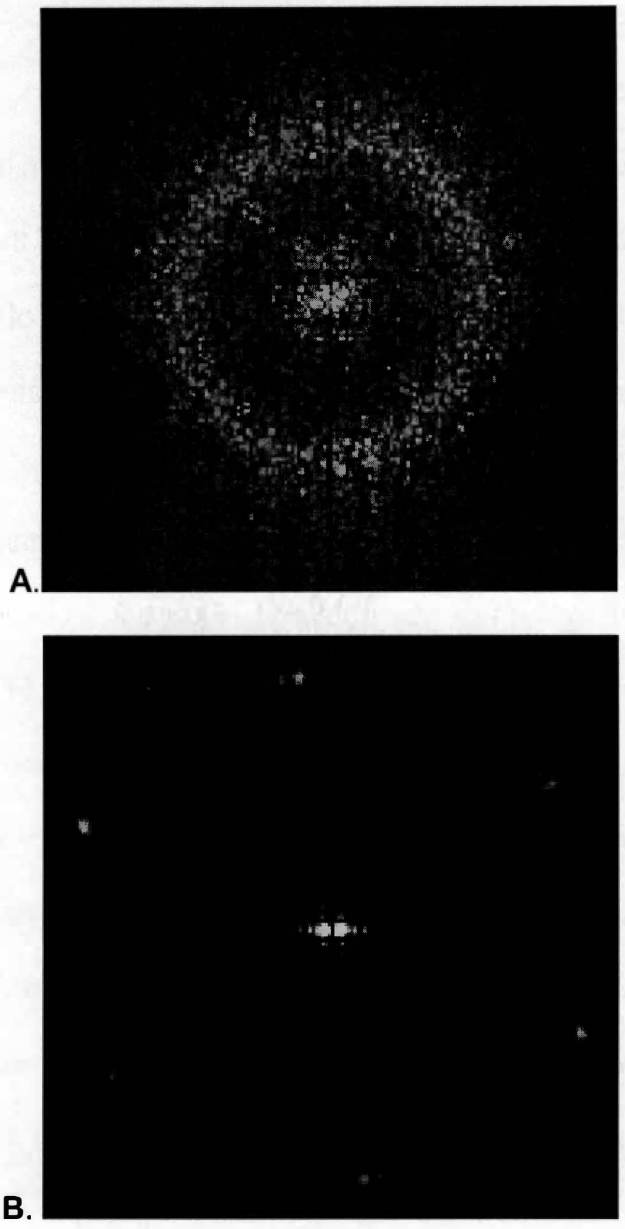

Figure 2.3: Fast Fourier Transforms of A). Non-ordered polymer template B). Highly ordered polymer template.

H. Scanning Electron Microscopy (SEM) & Energy Dispersive X-ray Analysis (EDX)

Formation of nickel nanodots and the growth of carbon nanofibers from them were confirmed using a Hitachi S4700 scanning electron microscopy (SEM) equipped with energy dispersive X-ray (EDX) analytical capabilities. A scanning electron microscope creates magnified images by using a beam of electrons. The electron beam comes from a filament that is most commonly a Tungsten hairpin gun. The filament is a loop of tungsten which functions as the cathode. A voltage is applied to the loop, causing it to heat up. The anode forms powerful attractive forces for electrons. This causes electrons to accelerate toward the anode. Some electrons accelerate right by the anode and down the column.[52] The electron beam is focused into a small probe and is rastered across the surface of the sample. The electrons interact with the sample and result in the emission of electrons from the sample surface as the electrons penetrate the sample. These emitted particles can be collected with a detector.[53]

Energy Dispersive X-ray analysis (EDX) is an accessory to the SEM which allows simultaneous non-destructive elemental analysis of the sample.[54] When the electron beam hits the sample it creates secondary electrons leaving thousands of the sample atoms with holes in the electron shells. If the "holes" are in the inner shells, the atoms are not stable. To correct this, the electrons from outer shells will move to the inner shells. The outer shells are at a higher energy state so moving down releases energy in the form of X-

rays. The X-rays emitted from the sample atoms are characteristic in energy and wavelength to the element of the parent atom, as well as which shells lost electrons and which shells replaced them. These sample signatures can be collected and analyzed to provide information on the elemental composition of the sample.

2.3 Synthesis of Polymers

ATRP is a pseudo-living free-radical polymerization that produces polymers with a low polydispersity. [55] A protected free radical end allows for easy synthesis of block copolymers. The first block can be synthesized and characterized to ensure it is of the correct molecular weight and composition before additional blocks are added and the order in which the blocks are added does not play a significant role. [56] The living free radical end stays active. The initiator used in this work is the monofunctional initiator p-Toluenesulfonyl Chloride. It is combined with the monomer and catalyst CuCl along with 2,2'-Dipyridyl in the ratio given below.

Monomer : Initiator : CuCl : 2,2'-Dipyridyl

X : 1 : 2 : 6

The target molecular weight determines the molar ratio of monomer used in the reaction. The target molecular weight divided by the molar mass of the monomer determines the number of moles of monomer required to produce a polymer with the desired molecular weight. This number is used in the molar ratio as X. The actual moles of monomer used is determined by dividing the grams of monomer by the molar mass of the monomer. The

moles of monomer and the molar ratio can then be used to determine the required moles of initiator and catalyst in the reaction. All chemicals are combined in a two neck round bottom flask and placed under nitrogen flow. The mixture is taken through 3 freeze thaw cycles using dry ice to ensure all air is removed from the flask. The temperature of the flask is raised by submerging in a hot oil bath. For styrene synthesis the temperature is raised to 120 ˚C for 24 hours. Methyl methacrylate synthesis requires only 95˚C for 8 hours. The solution will completely solidify when polymerization is complete due to the lack of solvent. The polymer must be dissolved in a good solvent such as toluene and crashed out into a poor solvent such as cold methanol. To ensure the complete removal of all the CuCl catalyst the sample must be redissolved and precipitated multiple times until the polymer is clean. The polymer is then dried in a vacuum oven overnight to remove any remaining solvent.

The addition of a second block is achieved by repeating the same procedure as described above while using the first block as the initiator for polymerization of the second block. It is sometimes difficult to get the first block to dissolve in the monomer for the second block due to the lack of solvent. If the polymer is unable to be dissolved in the monomer of the second block, a small about, (10% of the total weight) of biphenyl ether can be used as a solvent, this was not required in this synthesis.

Using the procedure described above a diblock copolymer of poly(styrene-b-methyl methacrylate) was synthesized. The first block to be

synthesized was the poly(methyl methacrylate) of a target molecular weight of 11,000. The initiator, catalysts and monomer were combined with the ratio described above in a 2 neck round bottom flask. The flask was exposed to 3 freeze thaw cycles and was then heated to 90 ˚C for 8 hours in an oil submersion bath. The resulting polymer was dissolved in toluene and precipitated into cold methanol and filtered to remove the remaining catalyst. The dried polymer had a number average molecular weight of 13,600 and a PDI of 1.11 determined by GPC.

This polymer was used as the initiator for the addition of the polystyrene block. The target total molecular weight was 62,000. Styrene monomer the PMMA (initiator) and catalyst were combined in a breakneck flask. No solvent was required to dissolve the PMMA initiator. The flask was cycled through 3 freeze thaws with vacuum evacuation after each step. The flask was sealed with a torch and placed in an oil bath at 120 ˚C for 24 hours. Once complete the polymer was dissolved in toluene, precipitated into cold methanol and filtered to remove the remaining catalyst.

GPC was used to determine the molecular weight of the polymer as described in section 2.8A Nuclear Magnetic Resonance spectroscopy (NMR) was used to determine its composition as described in section 2.8B. The copolymer has a M_n= 63,000 with a PDI=1.03 and f_{pmma}=0.21.

A random copolymer of styrene and methyl methacrylate was synthesized utilizing the TEMPO (2,2,6,6-tetramethyl-1-piperidinyloxy) based initiator, 1-Benxyloxy-2-(2,2,6,6-tetramethyl-1-piperidinyloxy) ethane provided

by Craig Hawker [10]. Utilizing this initiator results in a polymer that is end caped with an –OH functional group. The hydroxyl group will covalently bond to the native silicon oxide layer of silicon. The desired molecular weight was used to calculate the amount of initiator required by using equation 2.3. The correct amounts of initiator and monomers were added to a breakneck ampoule, cycled through 3 freeze and thaws to remove any air. The ampoule was sealed using a torch and placed in a 125 ˚C oil bath for 24 hours. The polymer was dissolved in toluene and precipitated into cold methanol. The resulting polymer was analyzed by GPC and NMR as described in sections 2.2A and 2.2B. The composition of the random copolymer is f_{ps}=0.55 with a 10,000 M_n, PDI = 1.2.

MW = (grams of monomer/moles of initiator) **(2.3)**

2.4 Template Preparation

A. Sample Preparation

Neutralization of the silicon substrate was achieved by one of two methods. Passivating the surface is achieved by placing the silicon wafer in a 3% hydrogen fluoride aqueous solution for 5 minutes to remove the silicon oxide layer. Immediately following the HF bath, the samples were rinsed with deionized (DI) water and immediately the polymer film was spin cast onto the wafer at the desired thickness. The second method to neutralize the surface was to deposit the –OH functionalized random copolymer on the substrate. A 1.5% solution of a random copolymer that is 55% styrene and 45% methyl methacrylate with a hydroxyl functional group on one end of the polymer

chain is spin cast onto a silicon wafer at 2500 rpm. The sample is then placed into a vacuum oven at 170˚C for 24 hours. Since the annealing temperature is above the T_g (glass transition temperature) of the polymer, the hydroxyl endgroup covalently bonds to the silicon oxide layer on the wafer and forms a chemically bound brush. The sample is removed from the vacuum oven and sonicated in toluene for 15 minutes to remove unbound polymer. Ellipsometry is used to confirm the presence of the brush by measuring the thickness of the silicon oxide layer prior to brush deposition, followed by measurements after brush deposition and subsequent removal of excess polymer. A uniform polymer brush thickness across the sample was determined to be 4-5 nm. Multiple measurements are made after a series of washing steps to insure that only the chemically bound copolymer brush remains. The brush creates a neutral surface for the diblock copolymer.

The diblock copolymer/toluene solutions of either 60,000 molecular weight or 230,000 molecular weight were prepared in the concentrations determined from Figure 2.1 to create a film thickness equal to the center to center interdomain spacing (L_0), which is 32 nm for the 60K MW polymer and 70 nm for the 230K polymer. The 60,000 molecular weight polymer was dissolved in toluene to create a 1.0% by weight solution corresponding to a film thickness of 32 nm at 2500 rpm. A 2.0% by weight solution was prepared using the 230,000 molecular weight polymer to achieve a film thickness of 70 nm at 2500 rpm. These solutions were spin cast onto silicon substrates that had been neutralized utilizing one of the two techniques described above.

After spin casting the samples were placed into a vacuum oven at 170˚C for a controlled length of time allowing the polymer chains to reorganized and form the perpendicularly oriented cylindrical microdomains that are required to create the nanoporous template. The samples were removed and allowed to cool to room temperature. They were then placed under 254 nm wavelength Ultra Violet light for 10 minutes to degrade the perpendicularly oriented PMMA cylinders. The degraded PMMA was washed away using a glacial acetic acid bath followed by rinsing with DI water, and were dried using compressed nitrogen. The removal of the PMMA cylinders creates a nanoporous polymer template. The ordering of the pores was determined by examination with AFM as described in section 2.2 F.

B. Template Specifications

PS-b-PMMA copolymer molecular weights determine the size domains of the polymers used. The 60K molecular weight copolymer has an interdomain spacing L_0 = 32 nm which is defined as the center to center distance of the cylinders. The cylinder diameter for this polymer is 18 nm. While the 230K molecular weight copolymer has L_0 = 70 nm and a cylinder diameter of 40 nm.

2.5 Graphoepitaxy

Silicon wafers were patterned using the custom photomask from Advance Reproductions Corporation. The pattern creates mesas of controlled widths that vary from 3μm to 20μm separated by troughs of equal width. (Figure 1) Using standard photolithography and plasma etching techniques as

described in section 2.2 E, the pattern was transferred into the silicon wafer. Plasma etching was performed on a Trion Reactive Ion Etcher using CF_4 plasma under 150 mTorr of pressure with a CF_4 gas flow of 75 sccm, (standard cubic centimeters per minute) and O_2 flow of 3 sccm. The height of the mesas (H) or etch depths were controlled by varying the time the wafer was exposed to the plasma with the etch rate of the instrument being 100 nm/min which was confirmed using AFM. The remaining Cr mask was removed from the silicon wafer using a chromium mask etchant purchased from Transene Company Inc. These patterned silicon wafers were used to make polymer templates following the procedure outlined in section 2.4

2.6 Solvent Annealing

Solvent annealing techniques were used to examine the ability of a solvent environment to improve the long range order in diblock copolymer templates. Polymer films were spin cast onto silicon substrates that had been neutralized via passivation or a random copolymer brush as described previously in section 2.4. These samples were placed in a toluene saturated chamber that consists of a crystallization dish half full of liquid toluene with the spin cast samples placed on a piece of glassware that is placed in the crystallization dish that is large enough to not be completely submerged in the toluene. The chamber is sealed off from the atmosphere using aluminum foil and stored at room temperature. The excess toluene vapor environment allows for solvent swelling of the polymer film which creates mobility for the polymer chains that enables polymer chain reorganization. Samples were

removed from the toluene rich environment at controlled time intervals and allowed to dry in air. The templates were then prepared by UV exposure and acetic acid wash to remove the PMMA phase producing a nanoporous template as described previously in section 2.4. These samples were analyzed with Atomic Force Microscopy to determine their long range order.

2.7 Nickel Nano-dot Formation

Polymer templates that were prepared as described in section 2.4 were coated with a layer of Nickel at ORNL using a Varian 3118 evaporator, equipped with an Airco Temescal e-beam and a CV-8 power supply; model STIH-270-2MB, Four Hearth Electron Beam Super Source. The metal that was evaporated was purchased from Alfa Aesar. Nickel thicknesses were varied by adjusting the exposure times for a set evaporation rate. To determine the optimal metal thickness samples were prepared with a range of metal thicknesses from 1/30 – 1 times the polymer film thickness.

Removal of the polymer template and overlaying metal was achieved by sonicating in toluene for 30 minutes. To insure the complete removal of all remaining polymer, samples were exposed to an oxygen plasma etch for 30 seconds using a Trion Reactive Ion Etcher (RIE). Samples were then examined for the presence of nickel dots with SEM and AFM.

2.8 Carbon Nanofiber Growth

Plasma enhanced chemical vapor deposition (PECVD) was used to grow vertically aligned carbon nanofibers (VACNFs) from the catalytic nickel nanodots. VACNFs were grown in a vacuum chamber originally evacuated to

a pressure of $<5x10^{-2}$ torr before gas flow. Acetylene (C_2H_2) with a gas flow of 25 sccm, (standard cubic centimeters per minute) was used as the gas source making the total pressure of the chamber during growth to be 3 Torr. The substrate temperature during growth was 700 ˚C. The DC plasma discharge was operated at 400 mA and ~500 V. Samples were all grown for one minute. Following growth the samples were examined by SEM.

Chapter 3

Long Range Order of Cylindrical Morphology Self-Assembled Diblock Copolymer Thin Films Using Graphoepitaxy

3.1 Graphoepitaxy of Cylinders

The microphase separation of diblock copolymers can be used to produce nanoscale templates. A major limitation of moving this technology from the laboratory to a commercial application is the inability to achieve long range ordering in the template. Since graphoepitaxy has shown promise in the improvement of the order in spherical domain polymer templates there is an application driven motivation to both understand and optimize the conditions that influence graphoepitaxial ordering of polymer systems. This chapter presents an exploration of the effects of the variation of substrate topography, both in terms of the height of the mesa, and width of the trough has on the order that can be achieved in cylindrical domain diblock copolymer templates when thermally annealed.

In an effort to improve the long range order of cylindrical domain polymer templates, a thin polymer film was spin cast directly onto a patterned substrate with a trough width of 3μm and a depth of 2.0 L_0. This sample was annealed at 170˚C to allow for chain mobility and reorganization that results in microphase separation. The sample was exposed to UV radiation and was treated with an acetic acid wash in order to remove the PMMA cylinders leaving a nanoporous template. The area in the troughs was examined by AFM. The result was a template that demonstrated an improvement in order

as seen in Figure 3.1C. The significant improvement of long range order suggests that the patterned substrate induced order by providing a hard edge that introduced translational order to the system during the annealing process. The improved order was observed across the entire width of the 3μm wide trough.

3.2 Order Parameter

In order to quantitatively analyze the improvement in ordering that was achieved by using graphoepitaxy, computer analysis of the template was used. The fast Fourier transform analysis of the AFM images of the template yields an equivalent structure in the associated reciprocal space, which may then be analyzed using the order parameter described below . Fast Fourier transforms provide a mathematical analysis of the image that is analogous to producing a diffraction pattern. From this "diffraction pattern" information on the order in the system can be obtained. Figure 3.1A is a FFT of a non ordered polymer template. The toroidal shape of the FFT indicates only local ordering, as there is no net confinement of the reciprocal space vectors associated with the real space structure and all the cylinders are a fixed distance apart but are oriented randomly. Figure 3.1C, represents a more well-ordered system where the cylinders are all a fixed distance apart, and are positioned at exact points relative to each other. However, a more quantitative method for describing the order is needed to quantify the effectiveness of graphoepitaxy to induce long range order in the diblock copolymer thin film templates.

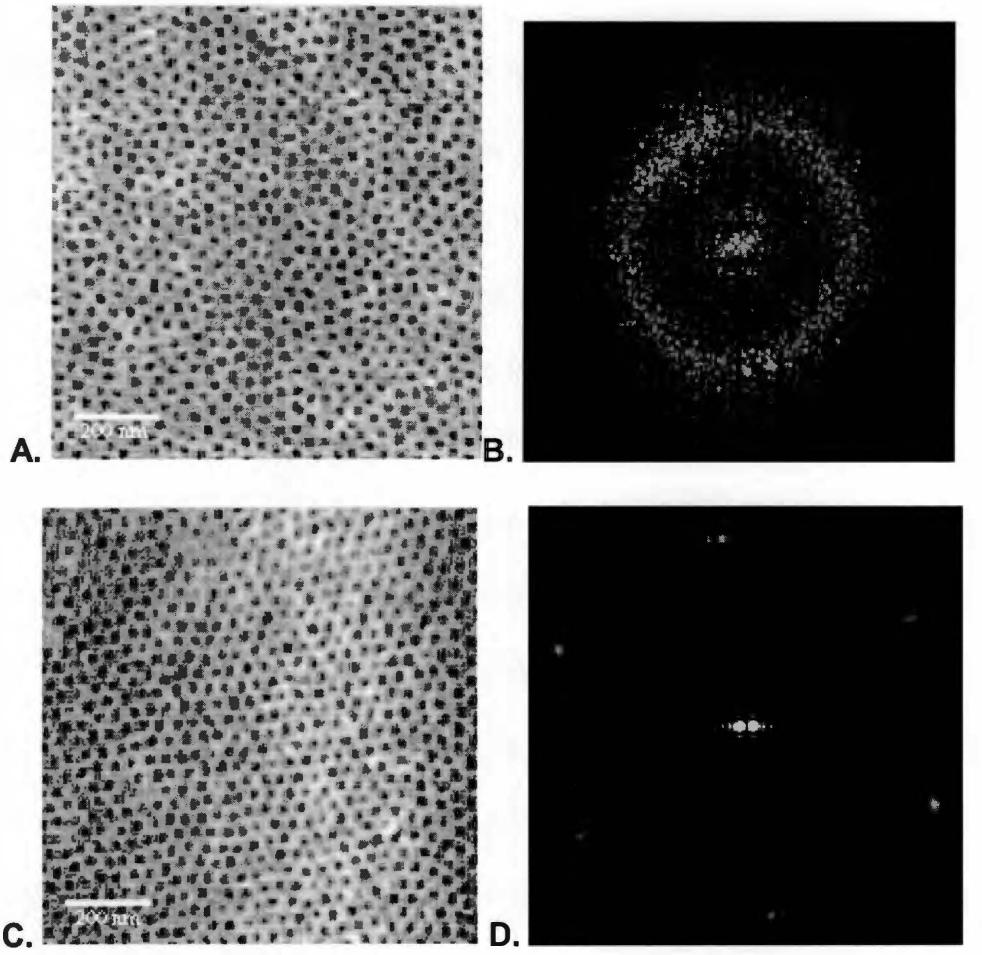

Figure 3.1: AFM images of 60K MW polymer prepared by spin coating. Images are 1 μm x 1 μm. **A.** Flat silicon substrate **B.** FFT image of A. **C.** patterned silicon substrate **D.** FFT image of C

Calculating an ordering parameter from the FFT provides a quantitative measure of the order present in the polymer template. An order parameter is often used when looking at crystalline structures, or alignment of molecules.[51] A completely disordered system has an order parameter of 0 while a perfectly ordered system has an order parameter equal to 1.

A computer program was written that converts the FFT image (Figure 3.2) into a plot of the radial average as arbitrary intensity vs. distance from the center in pixels. This provides an average intensity of all points at *x* distance from the center. This type of plot is often seen from small angle x-ray scatterning. From the radial average plot, the distance with the maximum intensity peak is identified. At the maximum intensity distance the azimuthal average of that distance ± 5 pixels is calculated and plotted as a function of intensity vs. azimuthal angle. From this plot the order parameter is calculated using equation 3.2 where I (q,ϕ) is the arbitrary intensity at a distance q and angle ϕ from the center, and $P_2(\cos\phi)$ is defined in equation 3.1.[57] These calculations were tested against a manufactured perfect system and imperfect system to ensure that a perfect system would provide an order parameter of one and an imperfect system would create an order parameter of 0.

$$P_2(\cos\phi) = \frac{1}{2}(3\cos^2 3\phi - 1) \qquad (3.1)$$

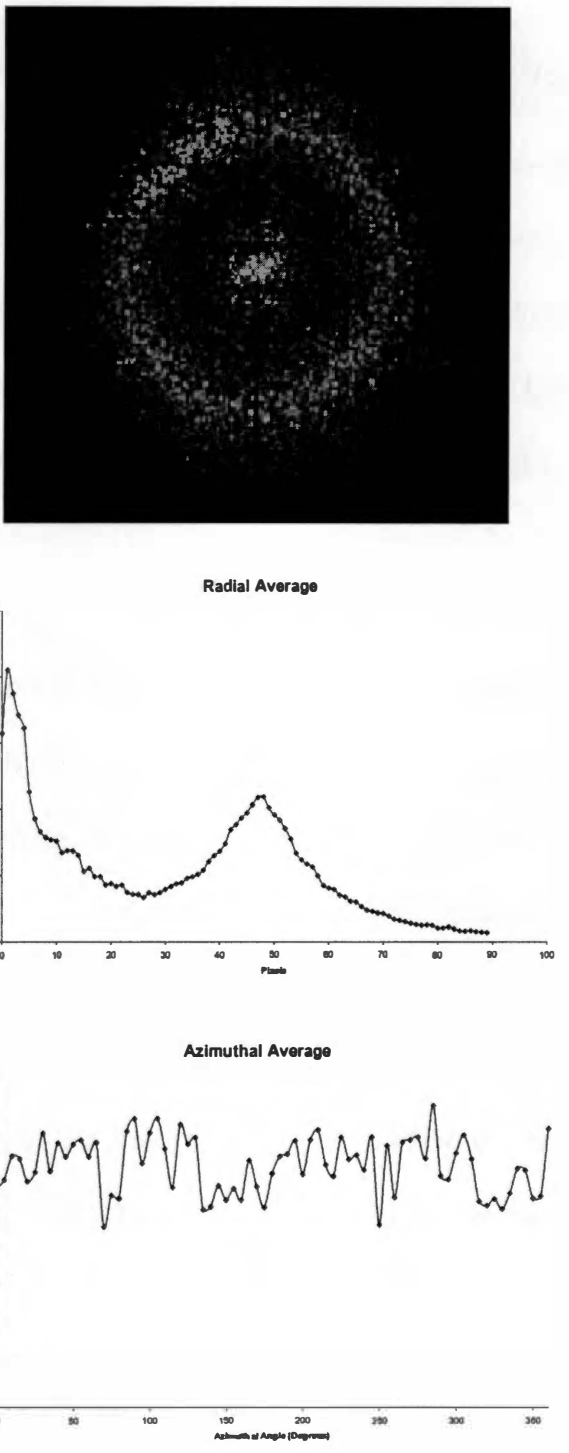

Figure 3.2: FFT of an unordered polymer template and its corresponding radial and azimuthal averages

$$\langle P_2(\cos\phi)\rangle = \frac{\int I(q,\phi)P_2(\cos\phi)\sin 3\phi d\phi}{\int I(q,\phi)\sin 3\phi d\phi} \qquad (3.2)$$

Using these equations the order parameter, the calculated order parameter for the unordered polymer template in Figure 3.1a, and Figure 3.2 is 0.013. The calculated order parameter for the highly ordered polymer template in Figure 3.1c, and Figure 3.3 is 0.914. It is noted that this functional form for the distribution of reciprocal space vectors is preliminary; further analysis which expands the reciprocal space structure in terms of cylindrical harmonics would provide an alternative method.

The error for the order parameter calculation is determined by calculating the order parameter for the 6 sections of 60 degrees each centered at each peak and averaging the order parameters from each section to determine the overall order parameter.

3.3 Vacuum Edge

From an application driven stand point it is imperative that a high level of ordering be achieved across the mesas as well as across the width of the troughs. It would be very impractical to create arrays that have half the area in a highly ordered array and the remainder in a nonordered array. It is therefore beneficial to be able to induce ordering not only in the troughs but on the mesas as well. In previous work by Segalman et al thinning at the mesa's vacuum edge led to the confinement of the spherical domain polymer microphases.[58] The spheres that are templated by the vacuum edge are a result of the surface energy of the polymer film at the mesa edge that forces

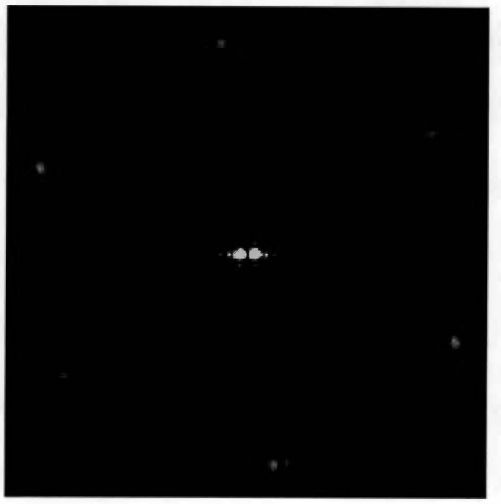

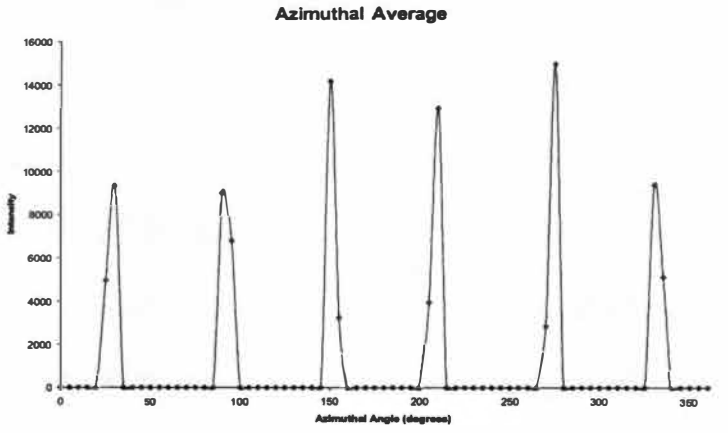

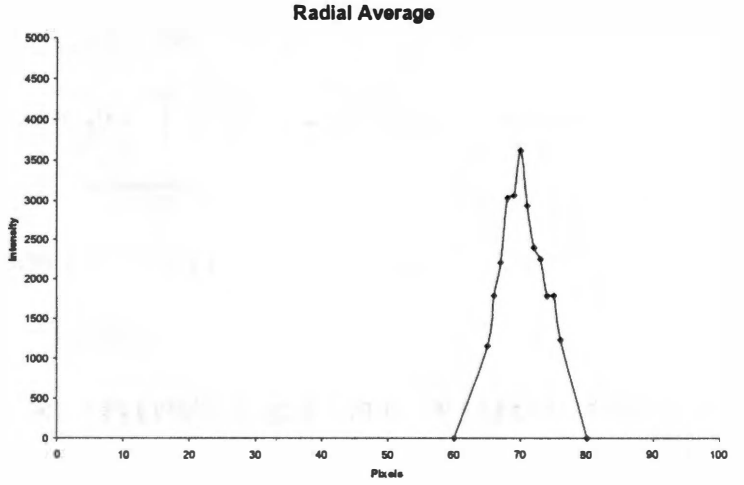

Figure 3.3: FFT of the ordered polymer template and its corresponding radial and azimuthal averages.

the polymer surface to be curved and compress the spheres closest to the edge. The curving of the polymer film near the edge reduces the surface area of the film, thus minimizing surface energy, and also reducing the thickness of the film. There is a minimum film thickness that a single sphere can fit into. Spheres have 3 finite dimensions that can be confined as the film thins. At the boundary thickness, a single row of spheres would be observed at a distance from the mesa edge.

A cylindrical system has an infinite length in the height dimension since is extends the entire length of the film so the thinning of the film is unable to confine a single row of cylinders as it does in the spherical system. Once the polymer film thickness is below the critical value to achieve a perpendicular orientation of the cylinders all order would be lost. Intuition suggests that there would be no ordering observed at the vacuum edge of the patterned silicon for a cylindrical system due to the formation of the cylindrical microphases being dependant on film thickness.[59] As the polymer film approaches the vacuum edge the thickness of the film is no longer in the appropriate range to form perpendicularly aligned cylinders.

This assumption is correct; the polymer film thins as it approaches the vacuum edge. The perpendicular orientation of the cylindrical microphase domains is lost as it approaches the mesa edge. However, there is an increase in the ordering across the mesas (Figures 3.4&3.5). As the polymer film thins, it is no longer in the appropriate range to form vertically aligned

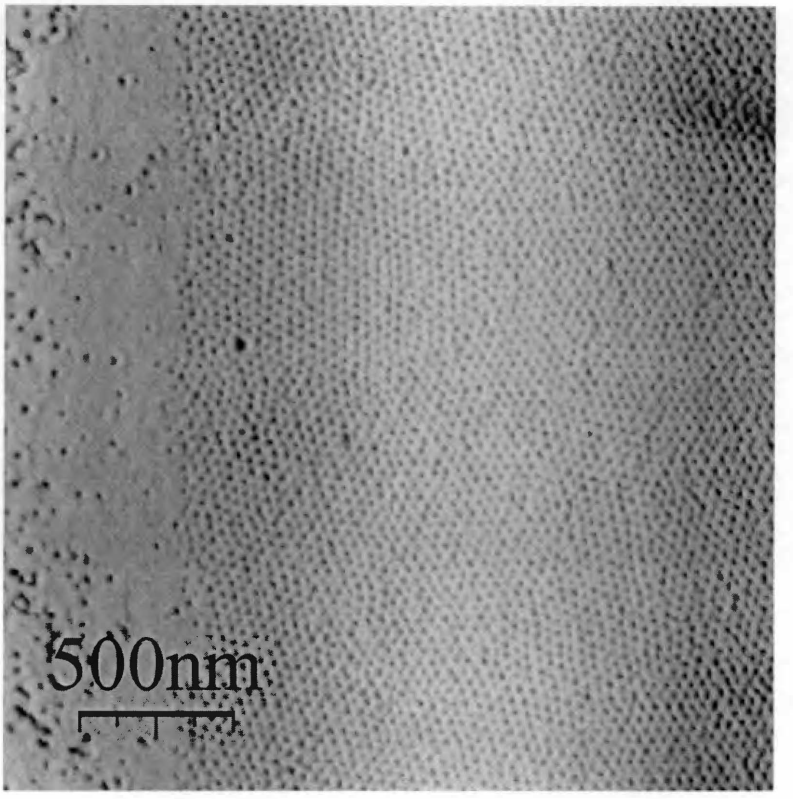

Figure 3.4: Phase contrast image from AFM scan demonstrating the order induced by the thinning of polymer film near the mesa edge of a sample prepared from 60K molecular weight polymer on a 2.0 L_0 mesa height patterned silicon substrate that has been annealed for 18 hours at 170˚C.

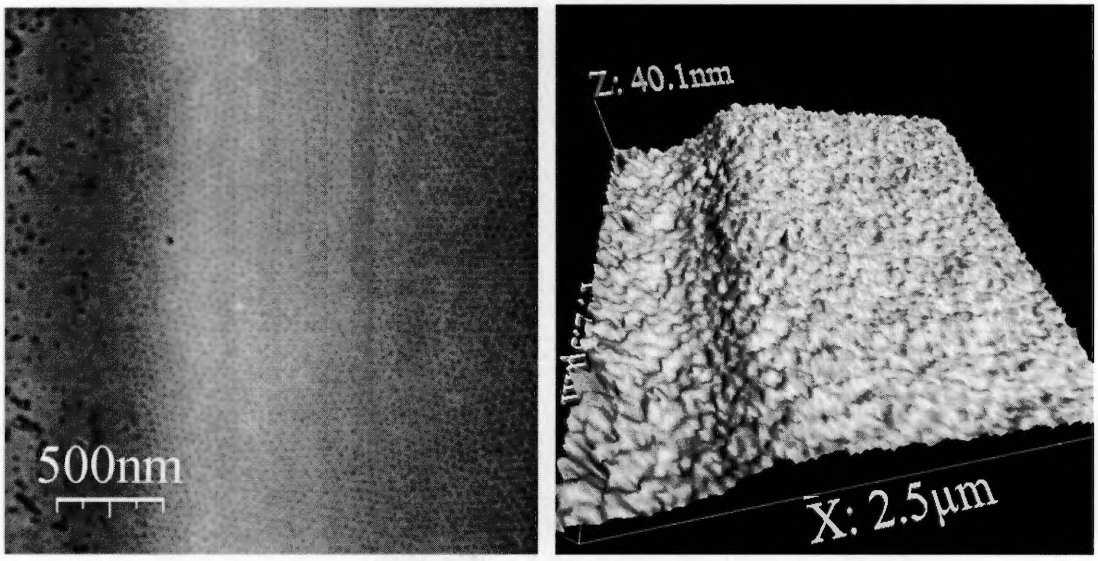

Figure 3.5: Height contrast AFM image along with its 3D image of demonstrating thinning of polymer film as it nears the mesa edge of a sample prepared from 60K molecular weight polymer on a 2.0 L_0 mesa height patterned silicon substrate that has been annealed for 18 hours at 170˚C.

cylinders. Therefore it pulls adjacent material in to achieve the critical film thickness and creates a terrace. This pulling of material behaves much like island or hole formation near the vacuum edge and creates a dramatic step in the polymer film as seen from the AFM image and 3D representation of Figure 3.5. The terrace is created to maintain a film thickness that creates the energetically most favorable vertical alignment of the cylinders. The straight edge of the mesa is maintained in the polymer film step and ordering is induced across the mesa. This is also demonstrated in the SEM image in Figure 3.6. The order parameter for the region on the mesa is 0.349 which is a significant improvement over the non-patterned polymer template sample which had an order parameter of 0.013.

3.4 Mesa Height Effect

Segalman *et. al.* observed an improvement in ordering of the polymer microdomains when the mesa heights were between 1.0 L_0 and 10 L_0.[58] In this work we examined mesa heights of 1.0L_0, 1.5 L_0, 2.0 L_0, 2.5 L_0, 5.0 L_0, and 10.0 L_0 to determine if there are any effect on the ordering of the cylindrical domain system. The width of the troughs as well as the polymer film thicknesses were held constant at 12 μm wide troughs, and 1.0 L_0 polymer film thickness. The samples were prepared with 60K molecular weight polymer that was templated with mesa heights ranging from 1.0 L_0 to 2.5 L_0 and annealed at 170˚C for 18 hours showed no difference in their ability to induce an improvement in ordering across the trough as seen in Figure 3.7. The calculated order parameters for these samples are 0.117 for

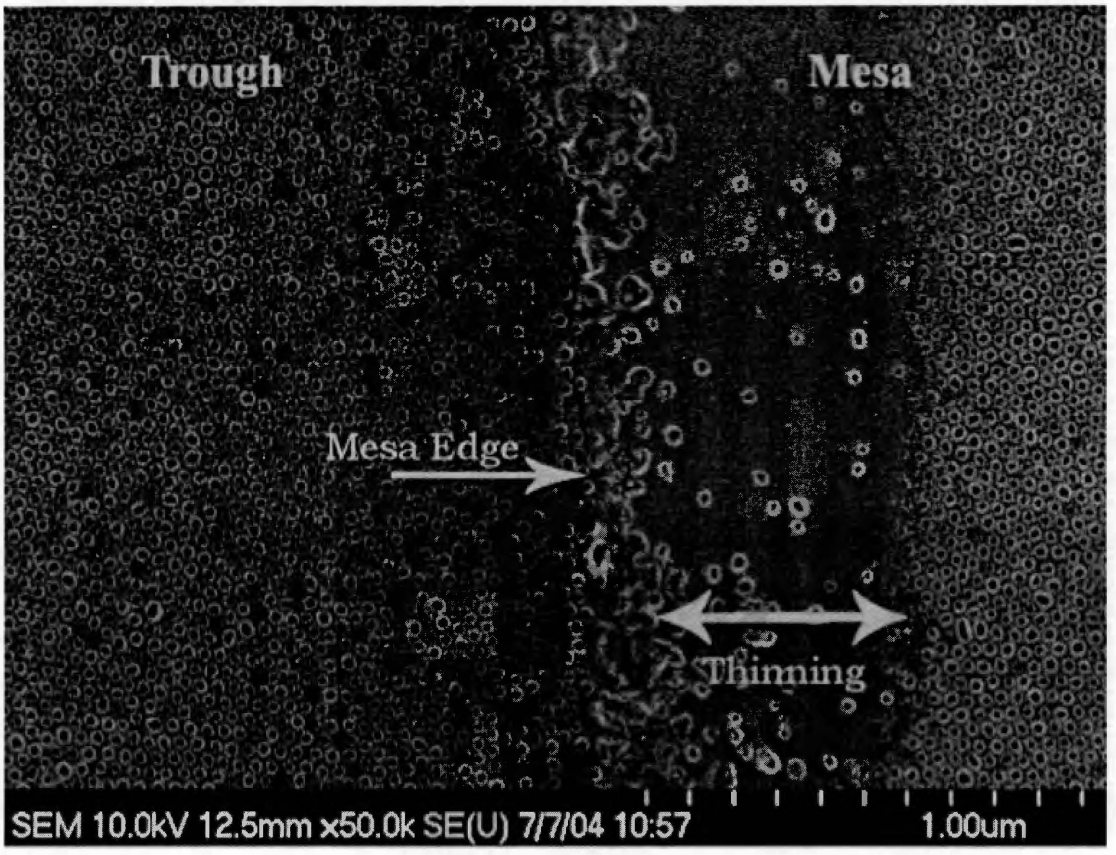

Figure 3.6: SEM image demonstrating thinning of polymer film as it nears the mesa edge of a sample prepared from 60K molecular weight polymer on a 2.0 L_0 mesa height patterned silicon substrate that has been annealed for 18 hours at 170˚C. Note the line of cylinders on the mesa that is parallel to the mesa edge.

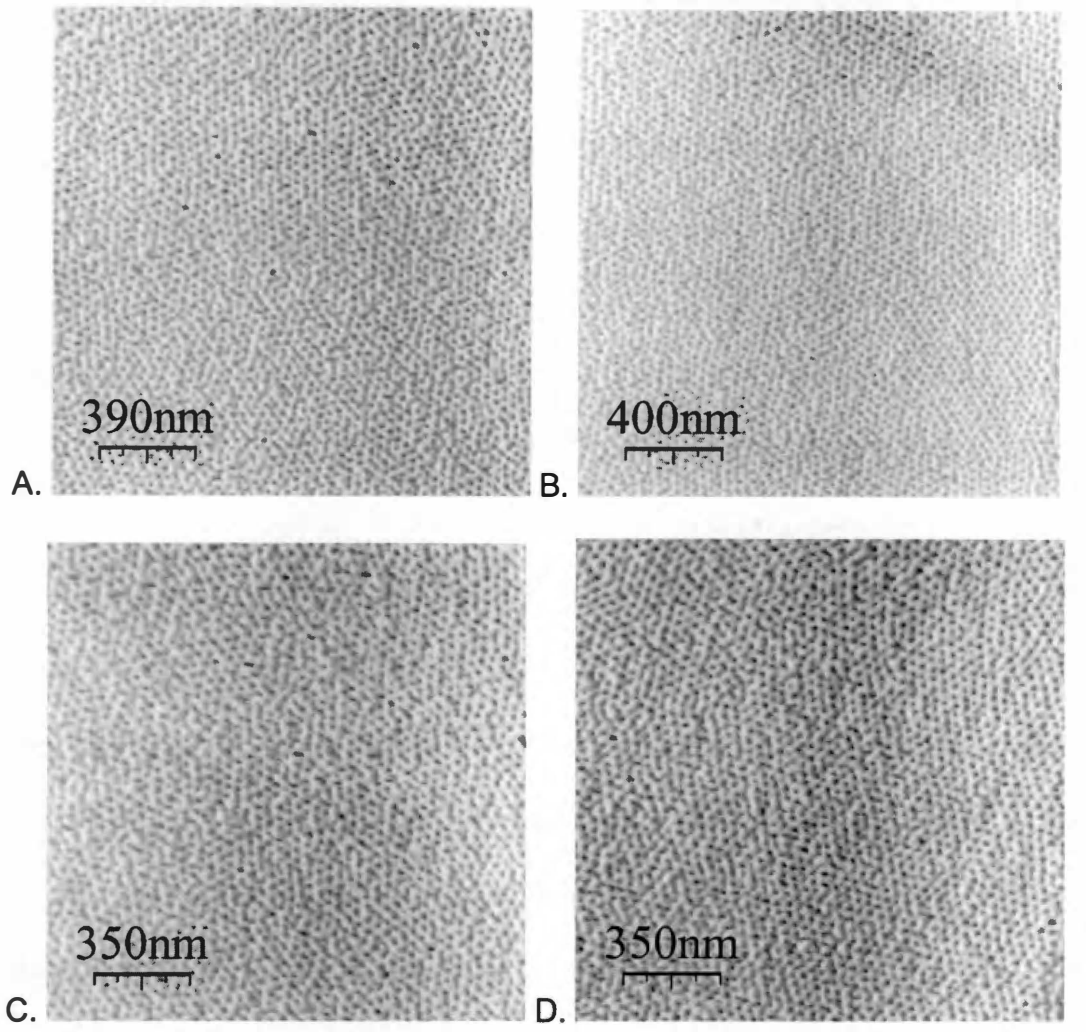

Figure 3.7: AFM phase contrast images ~2 μm x 2 μm of varying mesa heights in 12 μm troughs prepared with 60K molecular weight polymer and annealed for 18 hours at 170 °C. A). 1.0 L_0, B). 1.5 L_0, C). 2.0 L_0, and D). 2.5 L_0.

1.0 L_0, 0.415 for 1.5 L_0, 0.301 for 2.0 L_0, and 0.366 for 2.5 L_0. While all these samples were significantly more ordered than the polymer template prepared on the flat silicon substrate, those 1.5 L_0 and above were drastically improved from the minimum 1.0 L_0 sample which supports the theory that the mesa height must be at least equal to film thickness.

Mesa height of 10 L_0 was examined to determine the affect a mesa height significantly higher then the film thickness would have on the ordering. When samples were prepared with mesa heights of 10 L_0, and the 60K molecular weight polymer film spin coated onto the surface, and annealed at 170°C, ordering was observed on the mesa's and at the mesa edges in the troughs, yet the polymer film did not exhibit perpendicularly oriented cylinders across the width of the trough. This was most likely due to the inability to control the film thickness in the troughs during the spinning process. The ordering of the cylinders was confined to the area adjacent to the mesa walls. This can be observed in Figure 3.8. To determine if the cause of the loss of perpendicularly oriented cylinders was the result of the spinning of the polymer film onto the pattern substrate, samples were prepared by floating down the polymer film. Upon examination of these samples the same effects were observed as with the spin cast samples. Order was observed on the mesas and near the mesa walls in the troughs. Because there is some ordering of the microdomains adjacent to the mesa edge it demonstrates that the ordering of the cylinders can occur if the mesa edge is significantly higher than the polymer film. Significantly high mesas only limit the ordering of the

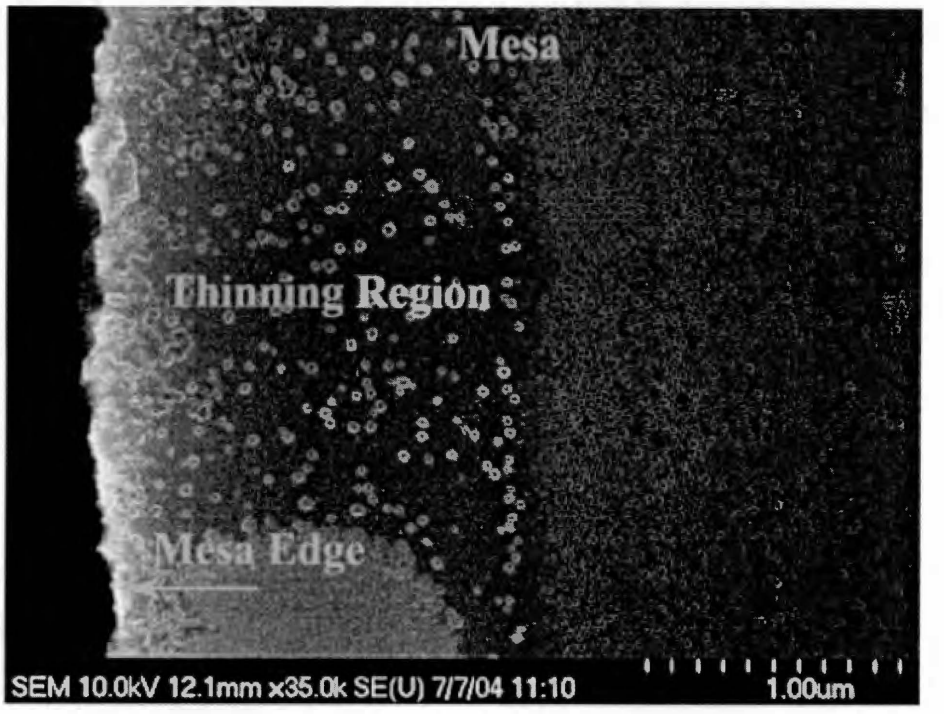

A.

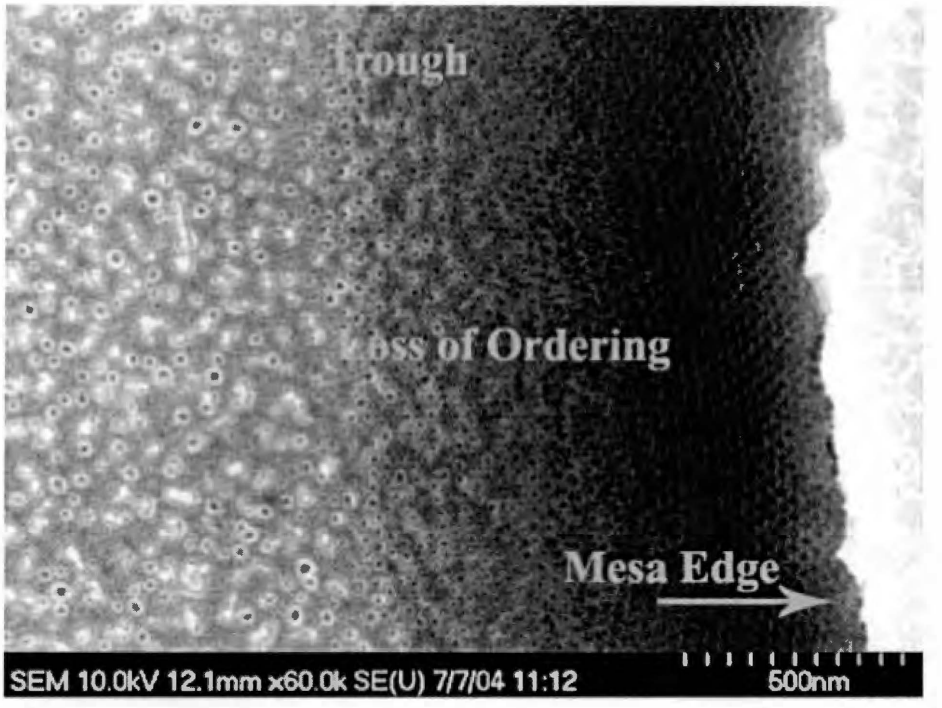

B.

Figure 3.8: SEM images of 60K mw polymer spin cast onto 10 L_0 mesa height patterned silicon sample and annealed at 170 ˚C for 18 hours. A). Image of the mesa that shows the order induced by polymer film thinning at vacuum edge. B). Order induced in trough only near mesa edge and lost further away from the edge.

polymer film across the width of the trough by their inhibition of the ability to control the film thickness.

Mesa height of 5.0 L_o was also examined prepared by both spin casting and floating. In these samples, the vacuum edge was able to induce order across the width of the mesas as observed on previous samples. However, in the troughs there were areas that showed a loss of the perpendicular orientation of the cylinders that was due to incorrect film thickness that is similar to the samples prepared on substrates with a mesa height of 10 L_0. These samples were much better than those prepared with a mesa height of 10 L_0. The height of the mesa limits the ability to form films of uniform thickness as the height is increased to above 5.0 L_0. From this data it appears that the optimal range for producing ordered arrays of vertically oriented cylinders by graphoepitaxy to be 1.0 – 5.0 L_0.

3.5 Trough Width

The goal of this work and others like it is to improve the order of polymer template systems over as long a range as possible to utilize this technique for real world applications. In this study we examined trough widths of 3, 6, 8, 10, 12, 14, 16, 18, and 20 μm to determine the maximum width over which we would see an increase in order. All samples were prepared using a 60K molecular weight polymer on templates that with mesa heights of 2.5 L_0 with polymer film thickness of 32 nm (1.0 L_0) annealed under vacuum for 18 hours at 170°C. From these experiments we observed an increase in order across the width of the troughs in all samples compared to

templates prepared on flat silicon substrates. As expected the order that was achieved at the hard edge was approximately equal for all trough widths. Figure 3.9 depicts the order parameter at the trough edge as a function of trough width. The order parameter was determined by $2\mu m^2$ AFM scans at the mesa edge. No trough width effect is observed which is consistent with the hard edge inducing an increase in order. The order parameter of these samples was also measured at the center of the trough. It was found that as the trough width increases the order at the center of the trough decreases. Figure 3.10 demonstrates the ratio of the order achieved at the center of the trough compared to the order achieve at the edge of the trough decreases as the trough width increases. The AFM scan size was 2 μm^2 therefore the order in the 3 μm wide trough was assumed to be uniform across the entire trough and thus had a ratio of 1. When the trough width was increased from 3μm to 20 μm, the order at the center of the trough was decreased by 60%.

These results support the theory that the hard edge induces order into the system and the order propagates toward the center of the trough. The 2-D hexatic to isotropic liquid transition should be a function of distance from the hard edge which has been observed in previous work.[60,61] Segalman et al reported in their work examining the effect of trough width on PS-PVP spherical domain block copolymer thin films ordered using graphoepitaxy, that the presence of a hard edge imparts translational and orientational order on a 2D array of block copolymer spheres. The effect dies away continuously as the distance from the edge is increased. They presented work that

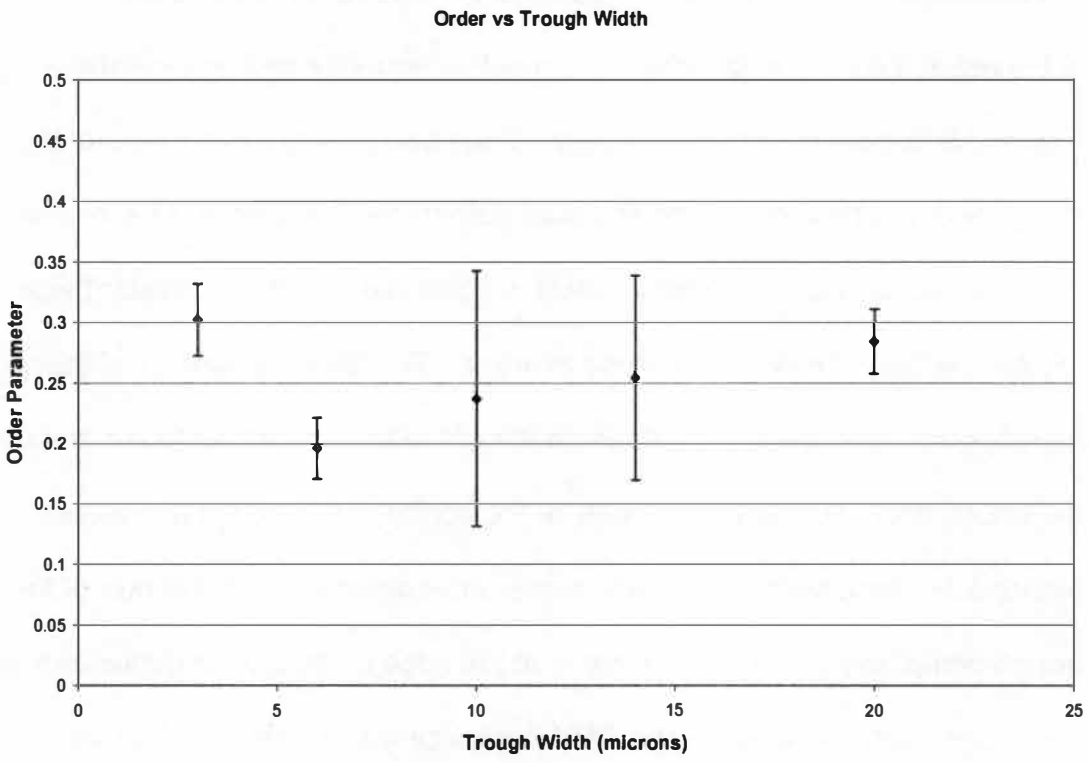

Figure 3.9: Order parameter at trough edge as a function of trough width of 60K molecular weight polymer templates prepared on patterned silicon substrate with a mesa height of 2.5 L_0 and annealed under vacuum at 170˚C for 18 hours.

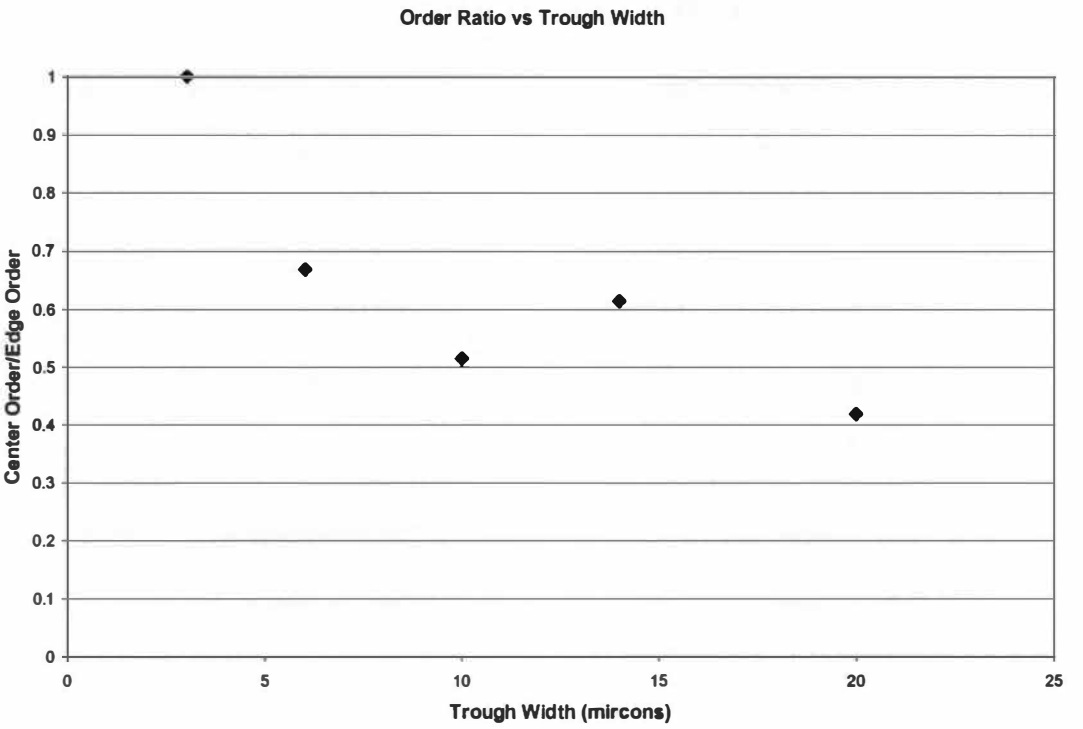

Figure 3.10: Ratio of the order parameter in the center of the trough divided by the order parameter at trough edge as a function of trough width of 60K molecular weight polymer templates prepared on patterned silicon substrate with a mesa height of 2.5 L_0 and annealed under vacuum at 170˚C for 18 hours.

suggested at the center of the trough is a liquid, but the presence of a hard edge resulted in an "edge freezing" of a hexatic layer. This is analogous to the surface melting or freezing of 3D crystals. In 3D systems the formation of this layer is driven by edge excess free energy $\Delta\gamma^* = \gamma_{el} - \gamma_{eh} - \gamma_{hl}$ where γ_{el}, γ_{eh}, and γ_{hl} are free energies of edge-liquid (el), edge-hexatic (eh), and hexatic-liquid (hl) interfaces. If the transition from hexatic to liquid is 2nd order as predicted by Halperin and Nelson then $\gamma_{hl} = 0$. The free energy of a block copolymer liquid-edge is greater than that of a block copolymer hexatic-edge. Therefore $\Delta\gamma^*$ should be a positive value and favor the edge freezing of a hexatic layer.

3.6 Molecular Weight

The use of diblock copolymer thin films as template formation shows promise as a method to evenly place nanoscale objects, however, there is very little information on kinetics of template formation, of long-range ordering or of molecular weight effects of these processes. To these ends the time evolution of the long-range order in templates formed from diblock copolymer thin films with two molecular weights is studied. This is accomplished by comparing the extent of long range order on both patterned (for grapho-epitaxy) and flat substrates by spin casting diblock thin films from toluene solution to create thin films that have a thickness that is equal to the center to center interdomain spacing (L_0) of the constituent microphase separated diblock copolymer. The patterned substrates have a mesa height of $1.5L_0$, as this pattern exhibited the most significant increase in order.[62] The samples

were annealed for times varying from 0.25 hours to 144 hours at a temperature of 170 °C for samples where the constituent diblock had number average molecular weights of 63,000 and 230,700, which will be denoted as 60K and 230K, respectively. Figures 3.11 and 3.12 show the change in the amount of long range order in the 60K and 230K samples, respectively, as measured by the order parameter, $\langle P_2(\cos \phi) \rangle$.

The evolution of long-range order in the 60K copolymer exhibits very interesting results. As expected, there is significant improvement in the ordering of the hexagonal cylinders in the polymer template relative to those that are prepared on a flat silicon substrate. Figure 3.11 depicts the improvement in the order parameter as annealing time increases. After annealing for just 15 minutes, formation of the hexagonally packed cylinders is observed since microphase separation occurs very rapidly, as this local process only requires relatively short-range motion of the chains. During the first 8 hours there is a steady increase in the order parameter from 0 to 0.176 as the chains have more time to execute the coordinated movement required to increase the order of the template. The mechanism of this motion must involve the motion of multiple chains, either individually or in a coordinated manner that results in the movement of a set of cylinders to create long-range order in the thin film. From 8 to 72 hours there is a further steady increase in the order parameter as further local ordering results in increased longer range ordering. After 72 hours there appears to be a leveling off in the order parameter as the system reaches its steady state order.

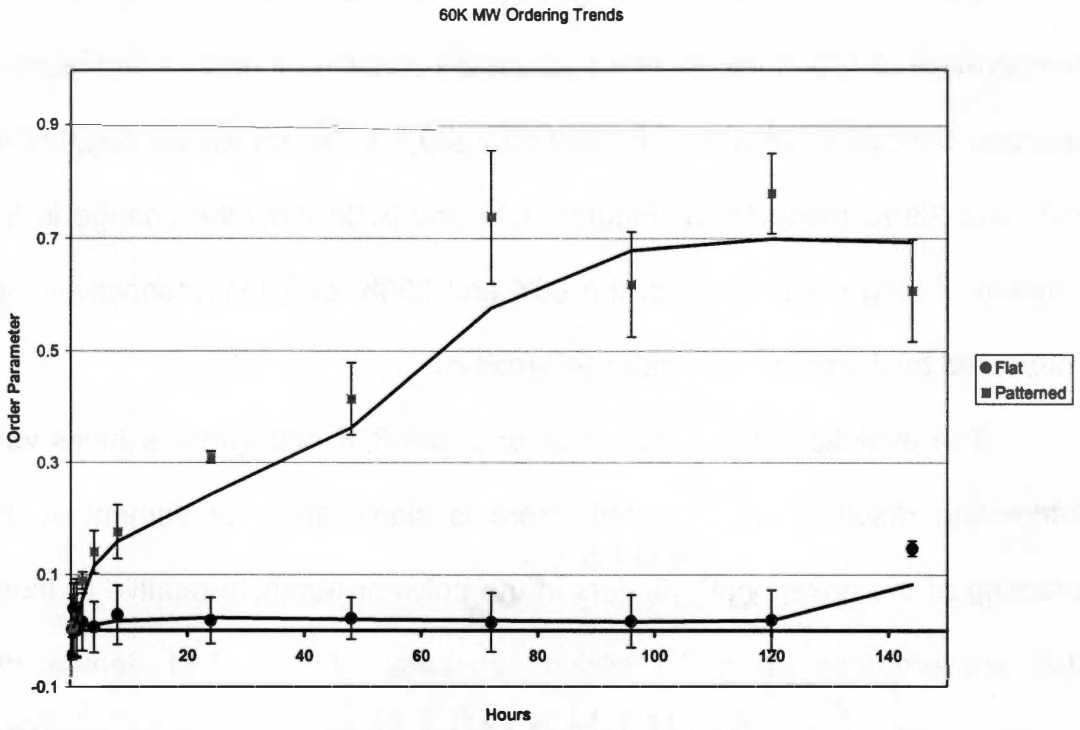

Figure 3.11: Graph depicting the evolution of the order parameter as annealing time increases for the 60K MW polymer. Samples prepared on a flat silicon substrate are depicted with circles. Samples that were prepared on patterned silicon are depicted with squares. The lines are added as a guide for the eye.

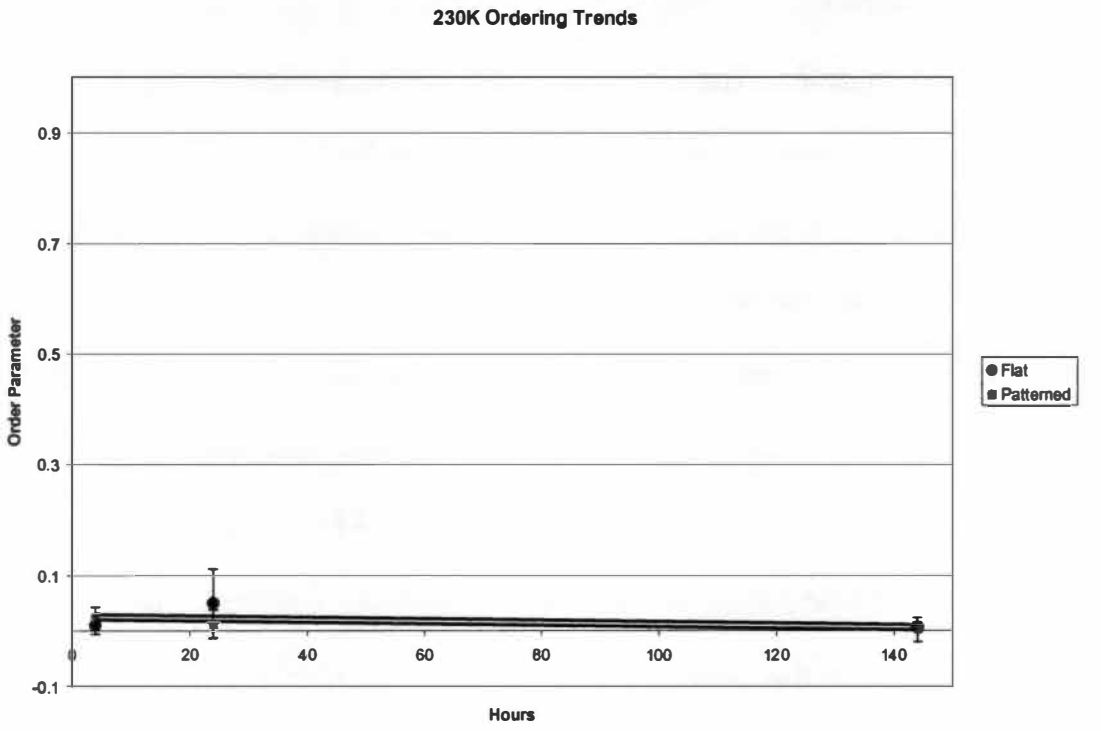

Figure 3.12: Graph depicting the evolution of the order parameter as annealing time increases for the 230K MW polymer. Samples prepared on a flat silicon substrate are depicted with circles. Samples that were prepared on patterned silicon are depicted with squares. The lines are added as a guide for the eye.

The samples prepared on flat silicon substrates did not show an improvement in order. The order parameter of the samples remains 0 within error for 120 hours of annealing. At 144 hours the order parameter of the system prepared on the flat surface does exhibit an increase in order, though only slightly. However, even if this is the beginning of a trend toward a more ordered system on the flat surface, these results demonstrate that the graphoepitaxy induced by the patterned surface provides a significant improvement in the driving force for ordering. The FFT images in Figure 3.13 demonstrate the increase in long-range order in the 60K samples with annealing time for the patterned and flat wafers. From this figure, it is also clear that after just 4 hours of annealing, the sample on the patterned silicon has significantly more order than those on the flat surface. After 144 hours the sample prepared on a patterned substrate has 6 distinct peaks, while the sample prepared on flat silicon only begins to show a the appearance of 6 peaks. Thus, these results indicate that the template prepared on a flat substrate does evolve towards a system with improved long-range order, but the evolution is very slow.

For the samples prepared using the 230K MW polymer, there is no change in the extent of long-range order observed in the thin film as the annealing time is increased from 4 hours to 144 hours. The order parameter remained very close to zero, signifying no long-range order in this sample. This was true for both the flat and the patterned silicon substrates.

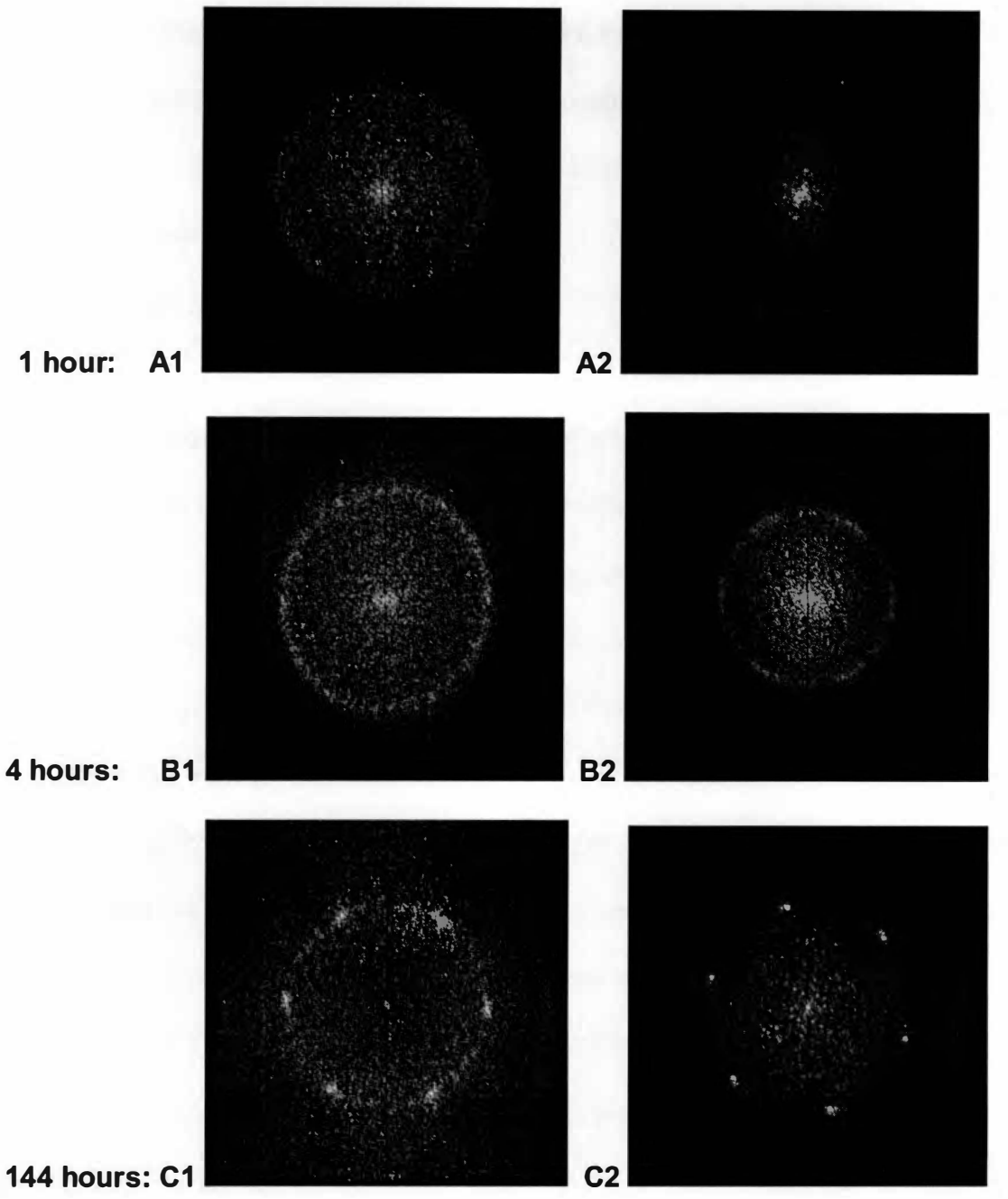

Figure 3.13: Fast Fourier Transform images as annealing time increases from 1 hour to 144 hours for 60K molecular weight samples prepared on flat silicon substrate (A1, B1, and C1) compared to samples prepared on 1.5 L_0 mesa height, 16 μm wide trough, patterned silicon substrates (A2, B2, and C2).

Figure 3.14 shows the FFT for the 230K polymer template prepared on a flat substrate and a patterned substrate that have been annealed for 144 hours, exhibiting no real difference between these two samples. This is in agreement with previous work in our lab that demonstrated that long range order in not attainable under these experimental conditions for large molecular weight polymers.[62]

This result is also consistent with the previous work reported by Xu et al. which examined the competition between the kinetics of microphase separation and the kinetics associated with ordering of microdomains normal to the surface.[59] Cylindrical domains with diameters between 14 and 50 nm in diameter were readily created in this study using microphase-separated copolymers with various molecular weights. However, when the molecular weight of the copolymer is increased to 295K, all lateral ordering of the cylindrical micro-domains perpendicular to the surface is lost for nanoporous templates prepared on flat substrates.[5] The extent and rate of microphase-separation in diblock copolymers is known to be controlled by the product, χN, where χ is the Flory interaction parameter between the two components of the diblock, and N is its degree of polymerization. As χN increases with molecular weight, the driving force for microphase separation increases and occurs very quickly for large molecular weight polymers. This may seem counterintuitive, as it is well-known that increased chain length slows down the dynamics of a polymer chain, which would suggest that longer polymer chains would microphase separate more slowly. However, microphase

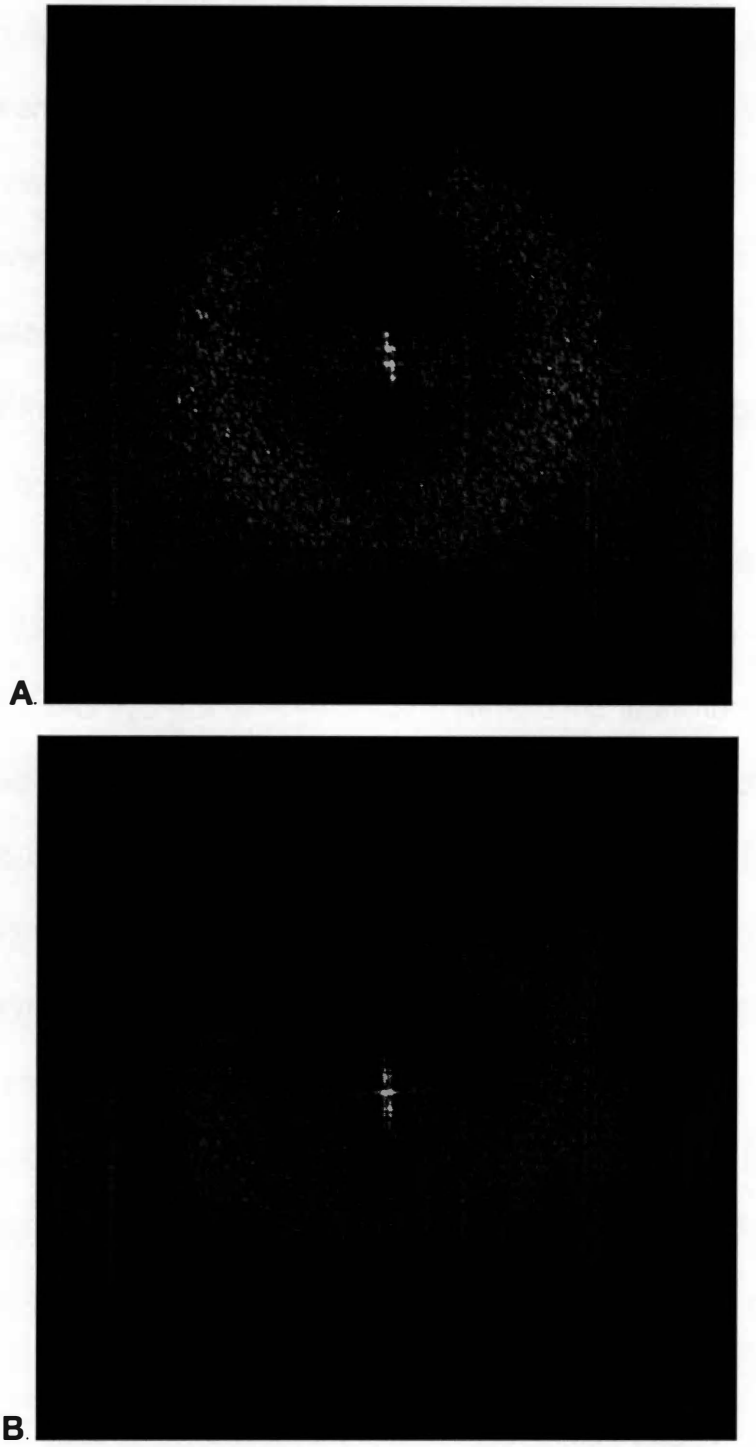

Figure 3.14: Fast Fourier Transform images of 230K MW polymer annealed for 144 hours prepared on A. flat substrate, B. 1.5 L_0 mesa height, 16 μm wide trough, patterned substrate. No difference is observed indicating no improved ordering from patterned substrate.

separation is a local process that only requires short-range motion of the chains.

Conversely, the ordering of the cylindrical micro-domains occurs much more slowly with an increased molecular weight, as this process requires the coordinated motion of many chains. Two possible molecular level processes for cylindrical domain reorganization include the motion of whole cylinders in the annealing process or the destruction and reorganization of the cylinders one chain at a time. The first method requires the coordinated motion of all chains comprising the cylinder, where the entire cylinder would migrate through the matrix as a single object. The second method involves the diffusion of individual copolymer chain lateral to the cylinders. In this case individual chains would diffuse through the matrix. In either case the improvement in order of the cylinders requires many chains to diffuse, either individually or as a group. This diffusion is progressively impeded as the molecular weight of the copolymer increases. Consequently, high molecular weight polymer thin films may become trapped in a non-equilibrium state on experimental timescales, due to the slow molecular motion of larger polymer molecules. This may result in a lack of long-range order in these thin films and result in the existence of a practical limit on the chain length that can be used to form nanoscale templates with long-range order.

As mentioned above, one molecular level process that can lead to the improvement of long-range order in the packing of the cylinders is the lateral self-diffusion of individual copolymer chains in the phase separated medium.

Inspection of the relative timescales needed for the molecular motion of the two polymer chain lengths examined here via this mechanism may provide insight into the factors that impact and limit the development of long range order in diblock copolymer thin films. The diffusion process of a single diblock copolymer in a microphase separated diblock copolymer system has a thermodynamic barrier, which is a result of the polymer chain experiencing an enthalpic penalty from mixing the two blocks during the diffusion process. Qualitatively, this enthalpic penalty retards diffusion, while the quantitative extent of the retardation depends on the microphase morphology, chain length, degree of entanglement, and the immiscibility between the blocks.[63] In the cylindrical morphology, two separate diffusion coefficients can be defined: D_{par}, which quantifies the rate the diffusivity of the polymer chain that occurs parallel to the cylinders, and D_{perp}, which quantifies the rate the diffusivity of the polymer chain across the microdomain interface. The formation of a highly ordered array would require self-diffusion that is perpendicular to the microdomains. The rate of this diffusion mechanism can be related to the unhindered diffusion of the copolymer chain by[63,64]

$$D_{perp} \sim D_0 \exp(-\alpha \chi N_{min}) \qquad (3.3)$$

Where χ is the Flory-Huggins interaction parameter, N_{min} is the degree of polymerization of the smaller block, D_0 is the diffusion coefficient of the copolymer chain in the absence of any interactions ($\chi \sim 0$), and α is a parameter on the order of unity. The equation demonstrates the exponential dependence of the decrease in copolymer chain diffusivity with χN_{min}. The

unhindered polymer chain diffusivity also scales with degree of polymerization:[65]

$$D_0 \sim N^{-2} \tag{3.4}$$

Finally, the distance that a polymer chain will diffuse (L_D) in a given time (t) is given by:

$$L_D = (4Dt)^{1/2} \tag{3.5}$$

Qualitatively, equations 3.3-3.5 imply that higher molecular weight diblocks will require significantly longer annealing times to achieve the same degree of ordering as a smaller chain, as the diffusivity of the larger copolymer is smaller due to both chain length and thermodynamic factors, while simultaneously, the required diffusion length will be larger due to the increase in interdomain spacing of the morphologies associated with longer chain lengths.

The comparison of the diffusive properties of the two molecular weights examined in this study can be quantified by using equations 3.3-3.5. If we first consider unhindered diffusion, the relative timescale of the motions of the two polymer chains can be determined using equations 3.4 and 3.5. N of the 60K copolymer is 595, while that of the 230K copolymer is 2275. Thus, from equation 3.4 the unhindered diffusivity of the 230K is 14.6 times slower than that of the 60K copolymer, as shown in equation 3.6.

$$\frac{N_{60}^{-2}}{N_{230}^{-2}} = \frac{D_{60}}{D_{230}} = 14.6 \tag{3.6}$$

To utilize equation 3.5 to determine a timescale of motion, a length scale must be chosen. As a minimum length that a chain must diffuse to create a new domain is the interdomain spacing, L_0 will be used as the targeted length scale of diffusion. Therefore, the ratio of times it takes the two copolymers to diffuse the length of the interdomain spacing is given by equation 5:

$$\frac{t_{230K}}{t_{60K}} = \left(\frac{L_{230K}}{L_{60K}}\right)^2 \frac{D_{60K}}{D_{230K}} \tag{3.7}$$

Substituting equation 3.6, L_{60K} = 32 nm, and L_{230K} = 70 nm into equation 5, shows that it takes 70 times longer for the larger molecular weight copolymer to diffuse between domains *unhindered* than the smaller copolymer. Thus, even without invoking thermodynamic slowing down it is clear that the ordering process in the thermal annealing of diblock copolymer thin films by graphoepitaxy will quickly become untenable as the molecular weight of the polymer chain becomes larger. Applying this factor of 70 to the data obtained from the 60K copolymer indicates that long-range order with an order parameter greater then 0.7 will require *at a minimum* annealing at this elevated temperature, for approximately seven months (5030 hours) for the 230K copolymer. Clearly, the thermodynamic penalty will further impede the coarsening of the diblock morphologies and thus these numbers must be viewed within this limitation.

This calculation agrees with the results observed in this study. The higher molecular weight copolymer does not exhibit any significant long-range

ordering in the timescales examined, up to 144 hours of annealing at high temperature. This result demonstrates a serious limitation to using graphoepitaxy to induce long range order in diblock copolymer thin films. Ideally, diblock thin films can be used to create templates of varying spacing and pore size, which can be controlled by the molecular weight of the copolymer. However, this set of results indicates that long-range order in the morphologies present in these thin films can only be induced by graphoepitaxy for smaller polymer chains, and thus well-ordered pores with only a narrow range of pore size and spacing is obtainable using graphoepitaxy.

3.7 Conclusions

It is important from an application driven stand point to improve the long range order of the diblock copolymer templates. However, the level of improvement that is required is dependant on the application. A balance must be achieved between the maximum order and cost effective processing. For high end applications such as data storage it may be necessary to achieve a order parameter that is 0.9 or better on a micron length scale. Conversely, it may only be necessary to have an order parameter of 0.2 if you are interested in creating a digital display that only requires an improvement in packing. Therefore, it is important to understand the parameters that allows for the tuning of the order parameter to create a system with the required long range order.

Chapter 4

The Use of Solvent Annealing to Improve the Kinetics of Ordering for Large Molecular Weight Diblock Copolymer Templates

This chapter examines the use of a toluene vapor rich environment to create vertically aligned cylindrical domain diblock copolymer templates from a PS-*b*-PMMA copolymer. The solvent annealing technique is also examined to determine if the rate of this method is sufficient to create long range order of high molecular weight copolymers. The kinetics of this ordering process are also compared to that of ordering by graphoepitaxy. Because this technique creates long range order rapidly it may be possible to access larger domain sizes by using larger molecular polymer systems then previously available. This, in turn, will enable the production of a wider range of array sizes and spacing for use in a wider range of applications that utilize diblock copolymer templates for patterning nanoscale objects.

Inspection of the relative timescales needed for the molecular motion via single chain diffusion provides insight into the factors that impact and limit the development of long range order in diblock copolymer thin films. The diffusion process of a single diblock copolymer in a microphase separated diblock copolymer system has a thermodynamic barrier, which is a result of the polymer chain experiencing an enthalpic penalty from mixing the two blocks during the diffusion process. Qualitatively, this enthalpic penalty retards diffusion, while the quantitative extent of the retardation depends on the microphase morphology, chain length, degree of entanglement, and the

immiscibility between the blocks.[63] In the cylindrical morphology, two separate diffusion coefficients can be defined: D_{par}, which quantifies the rate the diffusivity of the polymer chain that occurs parallel to the cylinders, and D_{perp}, which quantifies the rate the diffusivity of the polymer chain across the microdomain interface. The formation of a highly ordered array would require some polymer to diffuse perpendicular to the microdomains. The rate of this diffusion mechanism can be related to the unhindered diffusion of the copolymer chain by[63,64]

$$D_{perp} \sim D_0 \exp(-\alpha \chi N_{min}) \qquad (4.1)$$

Where χ is the Flory-Huggins interaction parameter, N_{min} is the degree of polymerization of the smaller block, D_0 is the diffusion coefficient of the copolymer chain in the absence of any interactions ($\chi \sim 0$), and α is a parameter on the order of unity. The equation demonstrates the exponential dependence of the decrease in copolymer chain diffusivity with χN_{min}. The unhindered polymer chain diffusivity also scales with degree of polymerization:[65]

$$D_0 \sim N^{-2} \qquad (4.2)$$

Finally, the distance that a polymer chain will diffuse (L_D) in a given time (t) is given by:

$$L_D = (4Dt)^{1/2} \qquad (4.3)$$

Qualitatively, equations 4.1-4.3 imply that templates formed from higher molecular weight diblocks will require significantly longer annealing times to achieve the same degree of long range ordering as those of a smaller chain,

as the diffusivity of the larger copolymer is smaller due to both chain length and thermodynamic factors, while simultaneously, the required diffusion length will be larger due to the increase in interdomain spacing of the morphologies associated with longer chain lengths. In chapter 3, we estimated that 230K diblock copolymer had an unhindered diffusivity that is 14.6 times slower than 60K diblock copolymer when both are ordered by graphoepitaxy.[66]

A recent method that has been introduced to improve the ordering of diblock copolymer templates is the use of solvent evaporation or solvent annealing. In this technique an improvement in ordering occurs by controlling the rate of solvent evaporation or by exposing the copolymer films to a solvent rich environment. This procedure is able to improve the order of the diblock copolymer template due to the solvent swelling the polymer matrix, which provides greater mobility of the polymer chains. The improved mobility of the polymer chains leads to the formation of highly ordered microdomains very rapidly. In recent work by Kim et al, a diblock copolymer of polystyrene-b-poly(ethylene oxide) (PS-b-PEO) was used to create a nanoporous template that was prepared using solvent annealing.[29] This technique was able to remove half of all defects in the template within 1 hour, while after 48 hours all defects had been removed from a 2 μm x 2 μm area. However, the solvent improves the mobility of the polymer chains to a level that the film will dewet if annealed too long.

One mechanism that is proposed to explain the development of long range order in solvent annealed diblock copolymer thin films involves the solvent swelling of the polymer film. For copolymers that contain immiscible blocks, the solvent mediates the non-favorable interactions between the blocks, allowing the copolymer to disorder. When the polymer film is solvent swollen, the glass transition temperature (T_g) is reduced to well below room temperature due to the increase in free volume. It is believed that as the solvent begins to evaporate at the polymer surface, the concentration of solvent decreases creating a solvent concentration gradient in the polymer film that is normal to the surface. (Figure 1.6) As the concentration of the solvent at the surface decreases, the microphase separation of the diblock copolymer should occur only at the surface. However, the copolymer deeper in the film is still in a disordered state due to the higher level of solvent concentration. It is proposed that long range order is introduced in the film by the propagation of order through the film from the surface as the solvent evaporates. The solvent gradient is highly directional which may lead to the formation of cylindrical domains that are well ordered and contain high aspect ratios as determined by the film thickness. [29]

Kim et al have demonstrated that solvent annealing is an effective technique to improve the long range lateral order of PS-b-PEO templates with benzene vapor.[29] This work examines the ability to improve long range ordering of PS-b-PMMA diblock copolymer templates with toluene vapor. An attractive aspect of this technique is its reduced sensitivity to film thickness

which allows for the production of ordered diblock copolymer templates that vary in polymer film thickness. The lack of sensitivity to the film thickness is a result of the proposed mechanism for ordering, which is the induction of order at the polymer air interface which then propagates toward the substrate. As a result the order is achieved regardless of substrate conditions, which was confirmed by Kim et al.[29] Despite this, all samples prepared for this work were prepared on random copolymer brush modified substrates, to maintain consistency with previous experiments[66,67].

High molecular weight (230K) diblock copolymer was spin cast onto a random copolymer modified silicon substrate from a 3.0% solution in toluene at 2500 rpm to achieve a film thickness of approximately 150 nm. The samples were immediately placed into a toluene rich vapor environment for 1, 4, 20, 48, 96 and 144 hours, removed and developed to form nanoporous templates. In this work comparisons will be made between diblock copolymer templates of the same molecular weight that are prepared via solvent evaporation (solvent), templates that are prepared by high temperature annealing on flat silicon substrates,(flat) and templates that are prepared by high temperature annealing on patterned substrates via graphoepitaxy (patterned).

The AFM scans in Figure 4.1 show the level of long range order in the cylindrical domains when solvent annealed at room temperature for 96 and when annealed at 170˚C for 96 hours. Figure 4.2 shows the evolution of the order parameter at different solvent annealing times in the templates. This

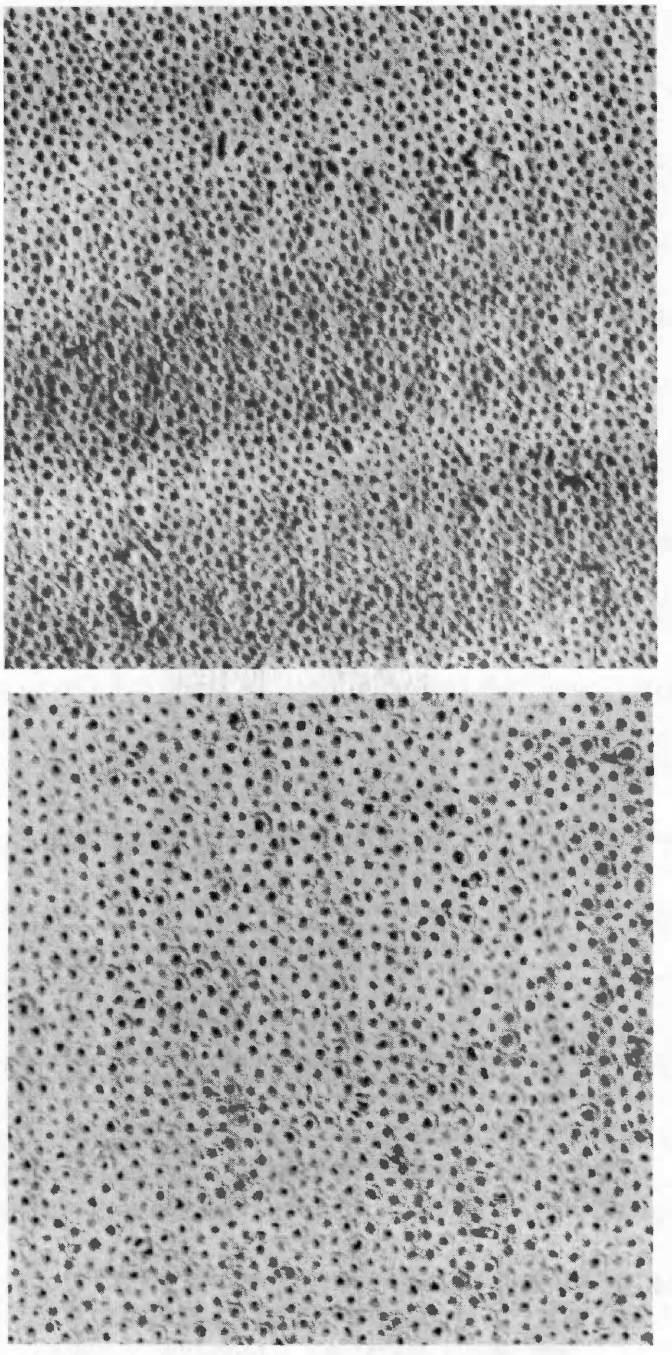

Figure 4.1: Phase contrast AFM images of 230K MW diblock copolymer annealed for 96 hours. Top: Annealed at 170˚C under vacuum. Bottom: Solvent annealed in a toluene rich environment at room temperature.

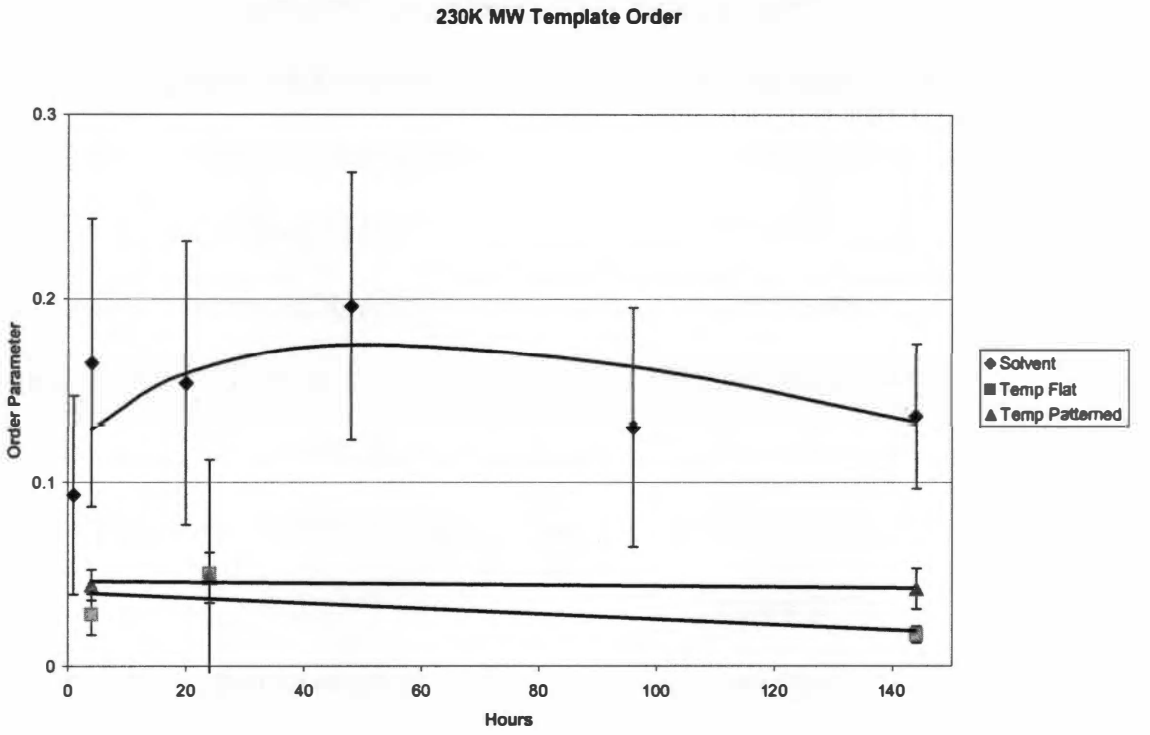

Figure 4.2: Diagram depicting the order parameter of a 230K molecular weight diblock copolymer template that has been ordered by varying techniques; Solvent annealing, Temperature annealed on flat substrates, temperature annealed on patterned substrates. The line is added as a guide for the eye.

evolution of long range order is compared to the long range order achieved for annealing on flat and patterned surfaces. Figure 4.2 shows that the order that is achieved when the templates are prepared by high temperature annealing on a flat surface as well as templates that are prepared on patterned substrates are not able to achieve an order parameter above 0.05. Templates that are prepared by solvent annealing were able to create templates with order parameters approaching 0.2. This order parameter is a significant improvement over standard high temperature annealing though well short of perfect order.

While this data demonstrates that solvent annealing improves the long range order, it is beneficial to provide further insight into the solvent annealing process and its impact on the diffusivity of the polymers in the diblock copolymer thin film. The development of long range order involves the diffusion of polymer chains, either individually or collectively through the polymer matrix. As a result the development of long range order is limited by the diffusion of polymer. By quantifying the development of long range order, an understanding of the diffusion of the polymer under different annealing conditions can be obtained.

Since microphase separation is a local process that requires only short range motion of the polymer chain, it will occur very quickly, requiring very little polymer diffusion. Once the microdomains are formed, long range ordering requires the diffusion of the entire polymer chain. A microphase separated diblock copolymer has an average interdomain spacing that is

determined by the length of the polymer chain which is controlled by its molecular weight. The average interdomain spacing (L_0) is the similar for oriented microdomains with long range order as well as without long range order. The difference between long range ordered templates and templates with no long range order is their positions relative to other local microdomains. In order to achieve long range ordering the microdomains must reposition themselves relative to each other to create an energetically most favorable state. This reorganization requires the diffusion of the microdomains as single chains or as whole objects through the polymer matrix. However the diffusion distance is on the order of L_0 or less because all microdomains in the template begin by being separated by an average distance equal to L_0. Therefore, the average distance that the polymer chains must diffuse to create long range order is proportional to the interdomain spacing of the polymer used to create the template, 70 nm for 230K and 32 nm for 63K. Thus as the distance that a copolymer must diffuse to induce long range order is on the order of L_0, this distance will be used when correlating the time of annealing to the diffusion of the copolymer using equation 4.3, i.e. $L_D=L_0$.

Without knowing the exact distance that the polymer chains are diffusing it is impossible to determine the actual diffusivity of the diblock copolymer in the templates. However, since the length of diffusion is proportional to the interdomain spacing of the polymer template it is possible to determine the relative rates of diffusion of the polymers. As the

development of long range order involves the diffusion of the polymer chain, it is possible to quantify the relative rates of diffusion of the polymers for different annealing conditions by analyzing the rates of development of long range order for different annealing conditions. Because the 230K molecular weight diblock copolymer template that was prepared on either a flat substrate or patterned substrate were never able to achieve an improvement in long range order, it is impossible to make a comparison between it and the template prepared via solvent annealing. Therefore, it is necessary to relate the dynamics of to the 63K molecular weight polymer that was able to achieve an increase in long range order by graphoepitaxy to the solvent annealed 230K template.

The maximum order achieved by the solvent annealed 230K MW sample was 0.196 which was achieved after 48 hours of solvent annealing. (Figure 4.2) In work presented in chapter 3, 8 hours of annealing was required for a 63K MW polymer sample that was prepared on a patterned template to create a template with long range order that has very similar to that of the 230K sample shown in Figure 4.3. Therefore, the ratio of diffusion time of the 230K copolymer that is solvent annealed to that of the 63K copolymer that is thermally annealed on a patterned surface is given in equation 4.4, where L_{60p} (interdomain spacing of 60K MW polymer prepared on a patterned substrate) is 32 nm and L_{230s} (interdomain spacing of 230K MW polymer prepared by solvent annealing) is 72 nm, and t_{60p} is 8 hours and

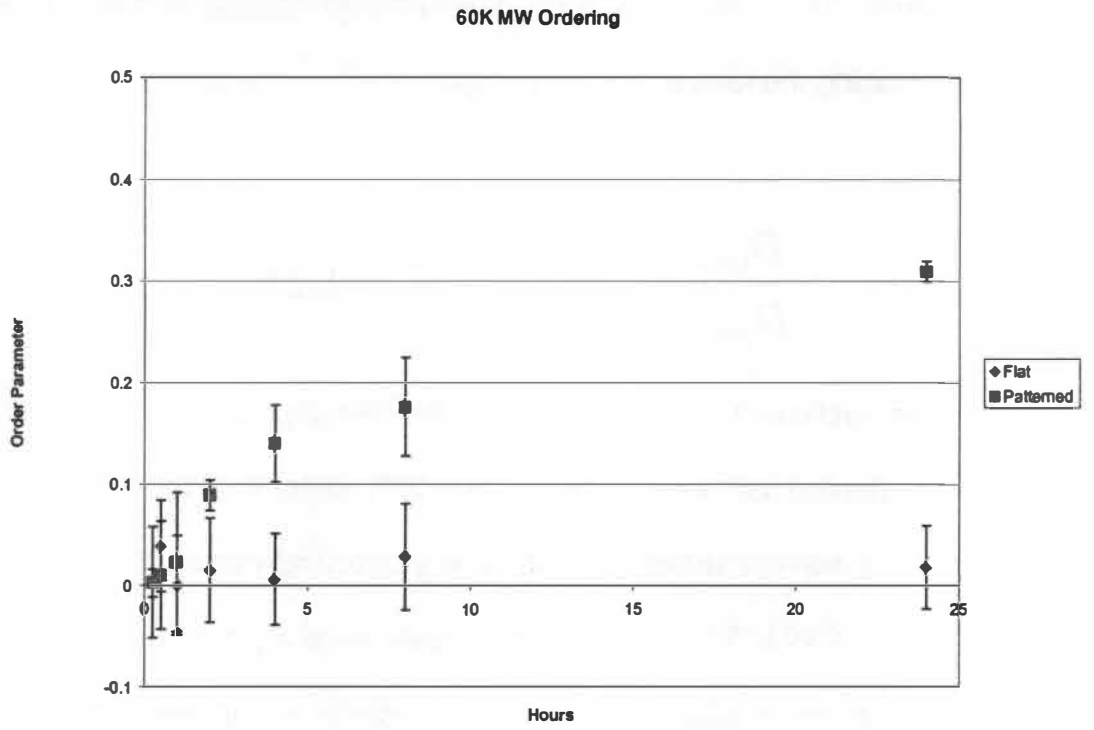

Figure 4.3: Graph depicting the evolution of the order parameter as annealing time increases for the 60K MW polymer. Samples prepared on a flat silicon substrate are depicted with diamonds. Samples that were prepared on patterned silicon are depicted with squares.

t_{230s} is 48 hours. This equation is derived by applying equation 4.3 to the two systems and taking the ratio of these two equations.

$$\frac{D_{60p}}{D_{230s}} = \frac{(L_{60})^2 4t_{60p}}{(L_{230})^2 4t_{230s}} = 1.25 \qquad (4.4)$$

This calculation indicates that the diffusion of the 63K copolymer annealed at 170°C on a patterned surface is approximately 25% faster than the 230K copolymer this is solvent annealed. This is very encouraging considering this diffusivity ratio of 63K to 230K when both samples were thermally annealed on a patterned substrate (D_{60p}/D_{230p}) is 14.6. From the two diffusivity ratios, (D_{60p}/D_{230s}) and (D_{60p}/D_{230p}) it is possible to calculate the diffusivity ratio of 230K templates prepared by solvent annealing to 230K templates prepared on patterned substrates (D_{230s}/D_{230p}), which is an order of magnitude higher (11.7).

It is also interesting to quantify the increased chain mobility of the copolymer by solvent annealing by identifying the temperature that would be required to create the mobility in the sample that is achieved by solvent annealing using time temperature superposition. This can be determined by correlating the friction factor (ζ) of the copolymer for each annealing process to the diffusion of the copolymer in each process. In equation 4.5, K_B is the Boltzmann constant, N is the degree of polymerization, d_T is the tube diameter of a reptating polymer, and b is the Kuhn length, which, except for d_T, are all

the same for both annealing processes, as it is the same polymer.[68] It is expected that the reptation tube diameter is increased by the presence of solvent molecules during the solvent annealing process. As the solvent molecules swell the polymer matrix they surround the individual polymer chains creating a local environment that the individual polymer chains can more easily move through.

$$\zeta = \frac{K_B T d_T^2}{3N^2 b^2} \frac{1}{D} \tag{4.5}$$

Taking the ratio of equation 4.5 for the solvent annealed template to that of the thermally annealed template gives equation 4.6.

$$11.7 = \frac{D_S}{D_T} = \frac{T_s}{T_T} \frac{\zeta_T}{\zeta_s} \frac{d_{Ts}^2}{d_{Tt}^2} \tag{4.6}$$

The results of equation 4.6, achieved by inserting the known annealing temperatures, 298 K for solvent annealing and 443 K for thermal annealing, show the change in the dynamics of the polymer chain when annealed by solvent. This change in polymer chain dynamics is due to changes in the local friction factor and changes in tube diameter as shown by equation 4.7.

$$\frac{\zeta_T d_{Ts}^2}{\zeta_S d_{Tt}^2} = 17.4 \tag{4.7}$$

The introduction of solvent molecules to the template swells the diblock copolymer thin film. This alters the local environment of individual polymer chains by surrounding them with small solvent molecules, which increases the reptation tube diameter. The small solvent molecules can be move more easily to allow for local polymer chain mobility which allows the individual polymer chains to move past each other with minimal friction because they are no longer tightly packed. As a result polymer chain reptation is improved which enables faster diffusion through the polymer matrix

If it is assumed that all improvement of dynamics occurs by lowering the friction factor, it is then possible to identify the temperature that would achieve the same lower friction factor that is achieved by solvent annealing at room temperature. In order to determine the required temperature to achieve the same friction factor the tube diameters are assumed to be equal. This is due to the fact that the tube diameters would be the same for the thermally annealed sample and the theoretical thermally annealed sample. While the tube diameter would not be equal for the solvent annealed sample, the effective temperature assumes thermal annealing therefore the tube diameter would be approximately equal. To make this correlation the temperature dependence of the friction factor must be known, which is given by the Williams-Landel-Ferry (WLF) equation (equation 4.8). In this equation C_1 and C_2 are taken from work by Lodge that examined the dynamics of PS/PMMA diblock copolymers.[68] The unitless values used for C_1 and C_2 are 7 and 125 respectively.

$$\log\frac{(\zeta(T_s))}{(\zeta(T_T))} = -\frac{C_1(T_S - T_T)}{C_2 + T_S - T_T} \qquad (4.8)$$

The solution to equation 4.8 indicates that solvent annealing at room temperature will provide the equivalent mobility to the copolymer as thermal annealing at 483 K (210°C).

These calculations shed light on the dramatic improvement of chain mobility and its result of long range order in diblock copolymer thin film templates by solvent annealing. Because solvent annealing drastically reduces the friction coefficient, higher molecular weight polymers are able to achieve an improvement in long range order that is not possible with other known ordering techniques. This can lead to the production of well ordered nanostructures from diblock copolymer templates with a wider range of sizes then thermal annealing. While the exact mechanism of the ordering process is still not completely understood, it is clear that this method is able to quickly produce diblock copolymer templates with long range order even for high molecular weight polymers.

Chapter 5

Using Self-Assembled Diblock Copolymer Thin Films to Template Nickel Nanodots for Carbon Nanofiber Growth

In this work the effectiveness of polymer templates formed from diblock copolymer thin films to produce VACNF from arrays of catalytic nickel dots is examined. One driving force for the creation of arrays of nanofibers with a high level of control of their size and spacing is that this control will enable the systematic examination of the effect of reduced dimensionality on the properties of the correlated magnetic and electronic structures that these particles may possess.[69,70] The use of polymer templates to create arrays of VACNFs could provide an ideal system to examine the effect of the size and spacing of the nanoparticles in an array on its magnetic or electronic properties.

For this study, templates were created from copolymers with two molecular weights. The diblock copolymer with the molecular weight of 230,000 produces template with 40 nm diameter pores that are spaced with a 72 nm center to center interdomain distance, while the diblock copolymer with the molecular weight of 63,000 produced 18nm pores and a 32 nm center to center spacing. To create the template from the diblock copolymer thin film, polymer films of PS-b-PMMA were spin cast onto a passivated silicon substrate creating a film that has a thickness that matched the interdomain spacing of the polymers; the 230,000 MW polymer formed films that ranged from 72-75 nm thick, while the 63,000 MW polymer was cast as films 31-32

nm thick. These thin films were then processed to remove the PMMA cylinders to create an array of nanopores as described in the experimental section. (Figure 1.4) Subsequent deposition of nickel and removal of the polymer template creates the desired nanoscale array of metal nanodots, which are then used as catalytic sites for the growth of carbon nanofibers.

In the course of the completion of these experiments, it became obvious that a variety of parameters dramatically impact the fidelity of the nanodot patterns and carbon nanofiber arrays. These parameters include the thickness of nickel deposited on the template, the surface treatment of the silicon surface, and the growth time of the nanofibers.

5.1 Nickel Deposition

The goal of the nickel deposition is to create a metal layer on and in the polymer template that will transfer the pattern of the template pores onto the silicon surface as metal dots. Initially, a layer of nickel that is $^1/_3$ as thick as the underlying polymer film was deposited as an initial attempt at nanodot array formation, as illustrated in Figure 1.7. Upon inspection of these nanodot arrays by SEM, it was found that dots were present on the substrate surface sporadically and with no effective order. This poor transfer of the porous template pattern onto the surface could be due to many factors. One possibility is that the deposited metal did not sufficiently penetrate the pores and contact the silicon surface during the evaporation procedure. This could be due to insufficient metal to reach the bottom of the pore. Alternatively, the nickel may remain in the pore when the polymer is lifted off, rather than

staying on the silicon surface. Previous work has reported the patterning of metal dots using similar templates, and therefore penetration of the pores by the deposited metal is known to occur in similar systems.

Alternatively, the poor transference of the nickel dots to the silicon surface may be due to the removal of the nickel with the polymer during the polymer template liftoff procedure. One possible reason for poor transference may be that the thickness of the metal is to large, resulting in strong adhesion to the template, especially on the pore walls. On removal, the nanodots are too strongly bound to the template wall and are therefore removed.

In order to test the dependence of the thickness of the metal film on the fidelity of pattern transmission, thin films of nickel that had thicknesses of 50 Á, 75Á, 100Á, and 125Á were deposited on the 70 nm thick 230K MW polymer film. Figure 5.1 shows the resultant patterns of nickel on the silicon surface. This figure shows that the thickness of metal that correlates to the optimal deposition of patterned dots is the nickel film that is approximately 100 Á thick. Unfortunately, even with this case, there was not complete transference of the polymer template pattern to the pattern of Ni dots for any pattern. For the 60K MW polymer template, which has a film thickness of 32 nm, Ni films with thicknesses of 25 Á, 40 Á, 50 Á, and 75 Á were examined, and the success of these metal films to transfer the template structure to the metal dots pattern is shown in Figure 5.2. For this copolymer thin film template, the transference of the polymer pattern to the nickel nanodot

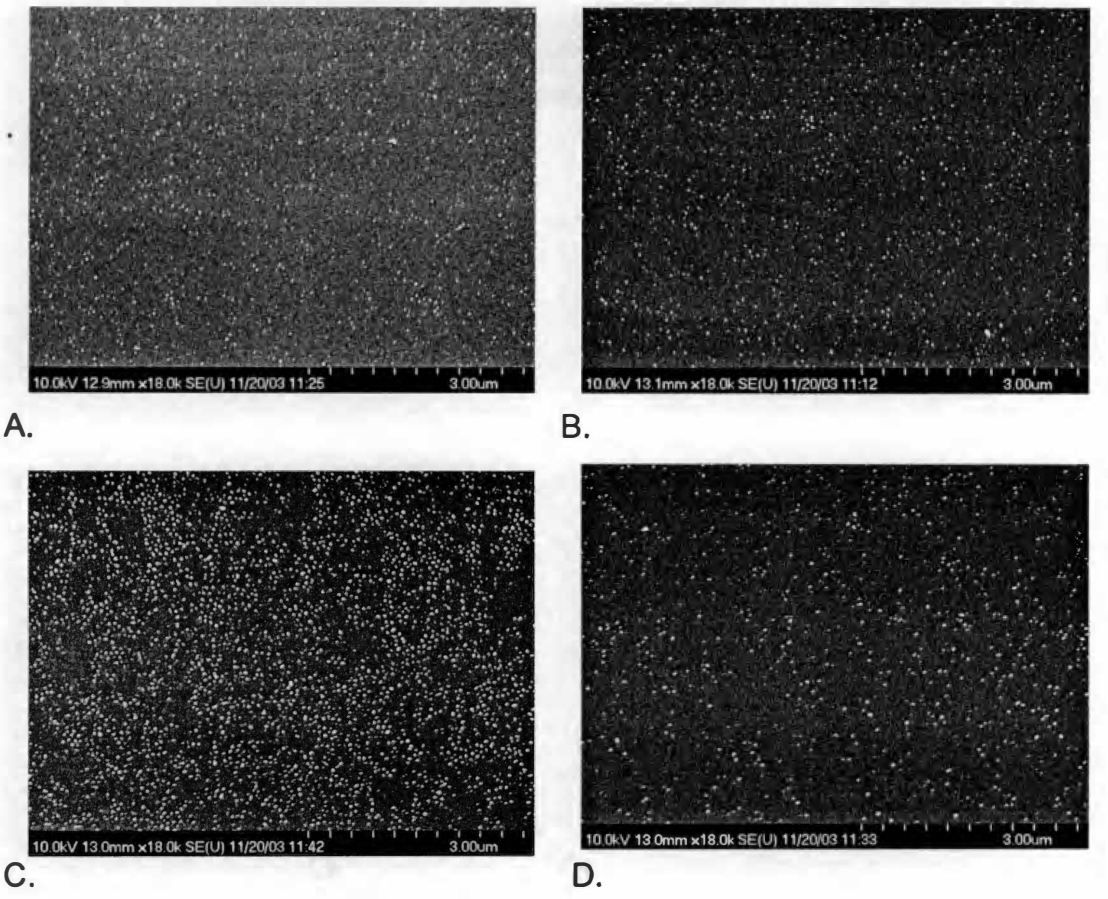

Figure 5.1: Nickel nano-dots templated by 230 K MW polymers 70 nm thick film. A) 50 nm thick nickel. B). 75 nm C). 100 nm D). 125 nm.

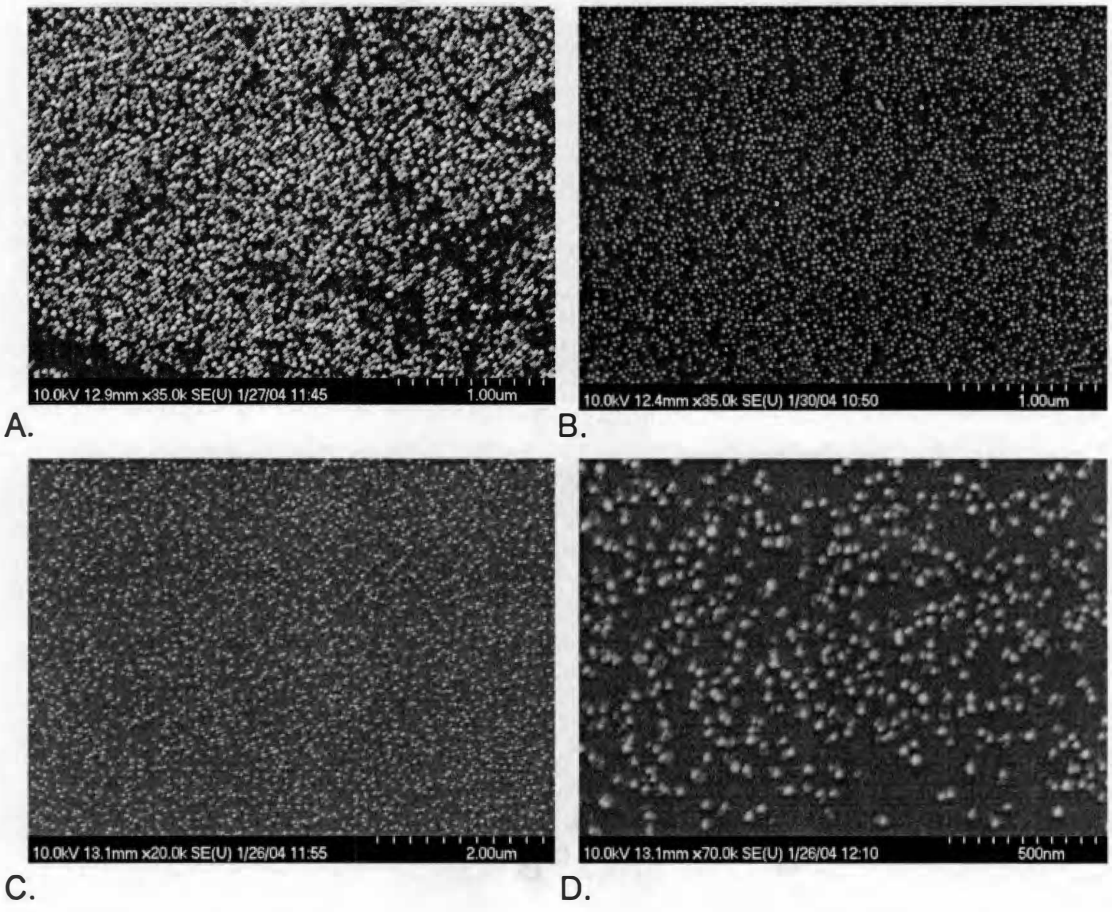

Figure 5.2: Nickel nano-dots templated by 60 K MW polymers 32 nm thick film. A) 25 nm thick nickel. B). 40 nm C). 50 nm D). 75 nm

pattern is much more complete and uniform over the 230K sample, but it is still short of 100%. The optimal thickness for this system appears to be 40 Å. It is interesting to note that for both copolymer templates, the ratio of the height of the metal film deposited to copolymer template thickness is ~1:8 for the optimal transference of the template pattern.

5.2 Silicon Surface Neutralization

To create the porous nanoscale template from the block copolymer thin film, the surface of the silicon wafer must be neutral to both components of the block copolymer.[5,10,67] Two methods to neutralize the silicon surface were examined in this study, removal of the native oxide layer on the silicon wafer with HF and the grafting of a random copolymer onto the wafer surface. The removal of the oxide layer with HF was used to produce the Ni nanodot arrays that are presented in Figures 5.1 and 5.2.

The impact of the neutralization procedure on the transference of the nickel nanodots to the silicon surface was also investigated. Thus, nickel nanodots were also deposited on a silicon surface that was passivated by the attachment of a hydroxyl functionalized random copolymer brush. The random copolymer brush coated substrates were prepared under the same conditions as previous samples except for the neutralization technique. This comparison was completed for the template produced from the 60K MW diblock. In this study, 10 Å, 20 Å, 30 Å, 40 Å, and 50 Å high films of nickel were deposited on the 32 nm thick diblock copolymer template. Figure 5.3

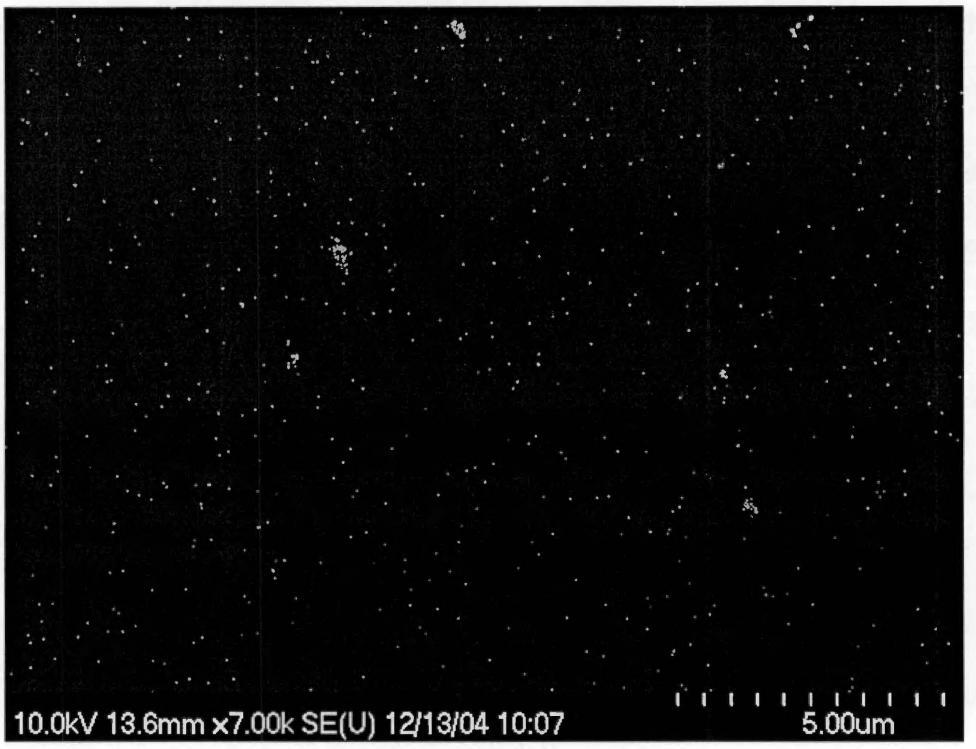

Figure 5.3: Nickel dots after liftoff prepared from a 60K diblock copolymer template. The template was prepared on a substrate that was neutralized via random copolymer brush.

shows that only a sporadic amount of Ni dots were present after liftoff when the templates were formed using this neutralization technique.

One possible explanation for the poor transference of the Ni on these samples is the response of the grafted copolymer brush during the liftoff procedure. As toluene is a good solvent for both PS and PMMA, the sonication in toluene step during template removal could impact the binding of the nickel to the copolymer brush during this procedure. As the brush is covalently bound to the substrate, this step will not remove the layer, but it is easy to envision it being swollen by the toluene and loosening the Ni nanodots from the surface, resulting in their liftoff during template removal.

5.3 Carbon Fiber Growth

Once the presence of the templated Ni nanodots was confirmed, carbon nanofiber growth was attempted using a chemical vapor deposition (CVD) growth procedure that is well established in the literature.[42,43,71] During the tip-type CVD growth process carbon diffuses into the catalytic nickel particle from all directions and a carbon coating is formed at the catalyst-silicon interface. This coating limits further diffusion of carbon at the catalyst-silicon interface, which creates a concentration gradient within the catalytic nanoparticle with very few carbon atoms at the catalyst-silicon interface, and many diffusing carbon atoms at the catalyst-gas interface with no carbon coating. This concentration gradient directs the carbon flow through the catalyst particle and the fiber grows.[43] After the catalyst is consumed, the carbon fibers will begin to etch back on themselves thus decreasing the

length of the fibers. Therefore, since the catalytic dots used in this work were smaller than any previously attempted the growth time was reduced to 1 minute in order to limit the back etching of the carbon fibers. A growth rate of 150 nm per minute is expected for this CNF growth procedure.[72] CNF growth was first attempted on the catalytic Ni that was patterned from the 230K MW polymer template. In this case the Ni dots were ~40nm in diameter. As seen in Figure 5.4 the growth was successful with reaction at all dots resulting in fiber growth. This success encouraged us to attempt to grow fibers from the 18 nm diameter dots that were patterned from the 60K MW polymer template. Again, fiber growth was observed with initiation from all dots. (Figure 5.5) These results demonstrate that carbon nanofibers can grow from Ni catalytic dots that are as small as 18nm in diameter, with tight packing of the catalytic dots.

It is clear that diblock copolymer templates are able to create nanoscale arrays of nickel nanodots, which, in turn, are able to catalyze the growth of VACNFs. This ability to control the size and spacing of the Ni nanodots enabled the growth of CNF from catalyst particles as small as 18 nm in diameter with center-to-center spacing of 32 nm. Neither the close proximity nor the limited catalyst particle diameter impedes the growth of the CNFs. Therefore, the use of diblock copolymer templates to produce patterned nanoarrays of carbon nanofibers may provide an avenue for the

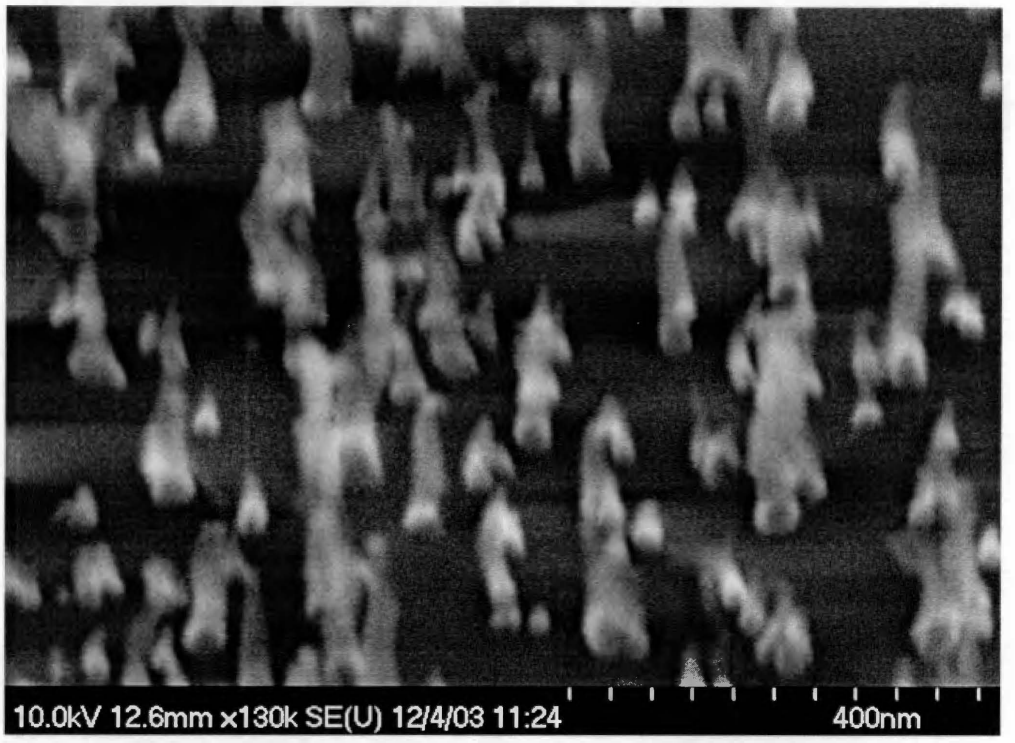

Figure 5.4: VACNF grown from 40 nm nickel dots patterned using 230K MW diblock copolymer template

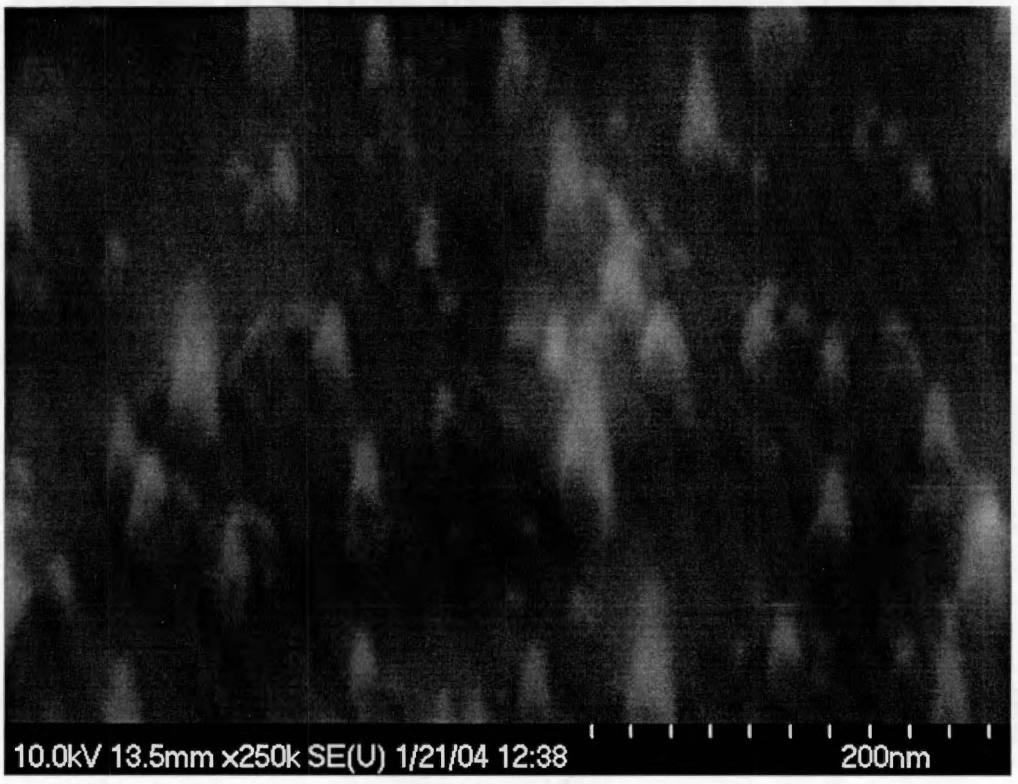

Figure 5.5: VACNF grown from ~18nm nickel dots patterned using a 60,000 MW diblock copolymer template.

production of nanoscale magnetically and electronically correlated systems. The complete transference of the pattern of the diblock copolymer thin film template to the nickel nanodots remains a difficulty that must be addressed in future work.

References

(1) Stevens, M.P. *Polymer Chemistry An Introduction*, Third ed.; Oxford University Press: New York, 1999.
(2) Datta, S. *Polymeric Compatibilizers: Uses and Benefits in Polymer Blends*, 1996.
(3) Park, C.; Yoon, J.; Thomas, E.L. *Polymer* **2003**, *44*, 6725-6760.
(4) Bates, F.S.; Matsen, M.W. *Macromolecules* **1996**, *29*, 1091.
(5) Xu, T.; Kim, H.C.; DeRouchey, J.; Seney, C.; Levesque, C.; Martin, P.; Stafford, C.M.; Russell, T.P. *Polymer* **2001**, *42*, 9091-9095.
(6) Leibler, Ludwik. *Macromolecules* **1980**, *13*, 1602-1617.
(7) Thurn-Albrecht, T.; Steiner, R.; DeRouchey, J.; Stafford, C.M.; Huang, E.; Bal, M.; Tuominen, M.T.; Hawker, C.J.; Russell, T.P. *Advanced Materials* **2000**, *12*, 787.
(8) G.Coulon; Russell, T.P.; Deline, V.R.; Green, P.F. *Macromolecules* **1989**, *22*, 2581-2589.
(9) Huang, E.; Pruzinsky, S.; Russell, T.P.; Mays, J.; Hawker, C.J. *Macromolecules* **1999**, *32*, 5299-5303.
(10) Mansky, P.; Liu, Y; Huang, E.; Russell, T.P.; Hawker, C. *Science* **1997**, *275*, 1458.
(11) Mansky, P.; Russell, T.P.; Hawker, C.J.; Pitsikalis, M.; Mays, J. *Macromolecules* **1997**, *30*, 6810-6813.
(12) Limary, R.; Green, P.F. *Mat. Res. Soc. Symp.* **2000**, *629*, FF1.5.1.
(13) Kim, H.C.; Russell, T.P. *Journal of Polymer Science. Part B, Polymer Physics* **2001**, *39*, 663.
(14) Fasolka, M.J.; Mayes, A.M. *Annual Review of Materials Research* **2001**, *31*, 323-355.
(15) T.L. Morkved, H.M. Jaeger. *Europhysics Letters* **1997**, *40*, 643.
(16) H.C. Kim, T.P. Russell. *Journal of Polymer Science. Part B, Polymer Physics* **2001**, *39*, 663.
(17) R. Limary, P.F. Green. *Mat. Res. Soc. Symp.* **2000**, *629*, FF1.5.1.
(18) R.A. Segalman, K.E. Schaefer, G.H. Fredrickson, E.J. Kramer, S. Magonov. *Macromolecules* **2003**, *36*, 4498-4506.
(19) H. Yokoyama, T.E. Mates, E.J. Kramer. *Macromolecules* **2000**, *33*, 1888-1898.
(20) Segalman, R.A.; H.Yokoyama; Kramer, E.J. *Advanced Materials* **2001**, *13*, 1152.
(21) Katzenberg, F.; Lieberwirth, I.; Petermann, J. *Journal of Materials Science* **1998**, *33*, 4787.
(22) Hahn, J.; Webber, S.E. *Langmuir* **2004**, *20*, 1489.
(23) Yi, S.S.; Moran, P.D.; Zhang, X.; Cerina, F.; Carter, J.; Smith, H.I.; Kuech, T.F. *Applied Physics Letters* **2001**, *78*, 1358.
(24) Segalman, R.A.; Hexemer, A.; Hayward, R.C.; Kramer, E.J. *Macromolecules* **2003**, *36*, 3272-3288.
(25) Halperin, B.I.; Nelson, D.R. *Physical Review Letters* **1978**, *41*, 121.

(26) Nelson, D.R.; Halperin, B.I. *Physical Review B* **1979**, *19*, 2457.
(27) Young, A.P. *Physical Review B* **1979**, *19*, 1855.
(28) Segalman, R.A.; Hexemer, A.; Kramer, E.J. *Macromolecules* **2003**, *36*, 6831-6839.
(29) Kim, S.H.; Misner, M.J.; Xu, T.; Kimura, M.; Russell, T.P. *Advanced Materials* **2004**, *16*, 226.
(30) Kimura, M.; Misner, M.J.; Xu, T.; Kim, S.H.; Russell, T.P. *Langmuir* **2003**, *19*, 9910.
(31) Fukunaga, K.; Hashimoto, T.; H.Elbs; Krausch, G. *Macromolecules* **2002**, *35*, 4406.
(32) Fukunaga, K.; Hashimoto, T.; H.Elbs; Magerle, R.; Krausch, G. *Macromolecules* **2000**, *33*, 947.
(33) Guillorn, M.A.; Melechko, A.V.; Ellis, E.D.; Simpson, M.L.; Bordonaro, G.J.; Merkulov, V.I.; Baylor, L.R.; Lowndes, D.H. *Journal of Vacuum Science &Technology B, Microelectronics and nanometer structures* **2001**, *19*, 2598.
(34) Baughman, R.H.; Zakhidov, A.A.; Heer, W.A. de. *Science* **2002**, *297*, 787.
(35) Lim, S.C.; Jeong, H.J.; Park, Y.S.; Bae, D.S.; Choi, Y.C.; Shin, Y.M.; Kim, W.S.; An, K.H.; Lee, Y.H. *Journal of Vacuum Science &Technology A, Vacuum, surfaces, and films* **2001**, *19*, 1786.
(36) Guillorn, M.A.; Simpson, M.L.; Bordonaro, G.J.; Merkulov, V.I.; Baylor, L.R.; Lowndes, D.H. *Journal of Vacuum Science &Technology B, Microelectronics and nanometer structures* **2001**, *19*, 573.
(37) Li, J.; Papadopoulos, C.; Xu, J.M.; Moskovits, M. *Applied Physics Letters* **1999**, *75*, 367.
(38) Huang, Z.P; Carnahan, D.L.; Rybczynski, J.; Giersig, M.; Sennett, M.; Wang, D.Z; Wen, J.G.; Kempa, K.; Ren, Z.F. *Applied Physics Letters* **2003**, *82*, 460.
(39) Park, M.; Chaikin, P.M.; Register, R.A.; Adamson, D.H. *Applied Physics Letters* **2001**, *79*, 257.
(40) Shin, K.; Leach, K.A.; Goldbach, J.T.; Kim, D.H.; Jho, J.Y.; Tuominen, M.; Hawker, C.J.; Russell, T.P. *Nano Letters* **2002**, *2*, 933-936.
(41) Ren, Z.F.; Huang, Z.P.; Wang, D.Z.; Wen, J.G.; Xu, J.W.; Wang, J.H.; Calvet, L.E.; Chen, J.; Klemic, J.F.; Reed, M.A. *Applied Physics Letters* **1999**, *75*, 1086.
(42) Merkulov, V.I.; Lowndes, D.H.; Wei, Y.Y.; Eres, G.; Voelkl, E. *Applied Physics Letters* **2000**, *76*, 3555.
(43) Melechko, A.V.; Merkulov, V.I.; Lowndes, D.H.; Guillorn, M.A.; Simpson, M.L. *Chemical Physics Letters* **2002**, *356*, 527.
(44) Eastwood, E.A. In *Chemistry*; University of Tennessee: Knoxville, 2002.
(45) Maldonado, Theresa. In ***http://www.uta.edu/optics/research/ellipsometry/ellipsometry.htm.***

(46) Zorich, Robert. *Handbook of Quality Integrated Circuit Manufacturing*; Academic Press Inc.: San Diego, 1991.
(47) Sze, S.M. *Semiconductor Devices Physics and Technology*; John Wiley and Sons: New York, 1985.
(48) Thompson, L.F.; Wilson, C.G.; Bowden, M.J., Eds. *Introduction to Microlithography*; American Chemical Society: Washington D.C., 1983.
(49) Baselt, David. California Institute of Technology, 1993.
(50) Round, Andy. ***http://spm.phy.bris.ac.uk/techniques/AFM/***, *University of Bristol*.
(51) Hongladarom, K.; Ugaz, V.M.; Cinader, D.K.; Burghardt, W.R.; Quintana, J.P.; Hsiao, B.S.; Dadmun, M.D.; Hamilton, W.A.; Butler, P.D. *Macromolecules* **1996**, *29*, 5346-5355.
(52) Chumbley, Prof. Scott. ***http://mse.iastate.edu/microscopy/home.html***.
(53) Petrova, Vania. ***http://cmm.mrl.uiuc.edu/techniques/sem.htm***.
(54) Seal-Laboratories. ***http://www.seallabs.com/edx.html***.
(55) Patten, T.; Matyjaszewski, K. *Accounts of Chemical Research* **1999**, *32*, 895.
(56) Eastwood, E.A.; Dadmun, M.D. *Macromolecules* **2001**, *34*, 740-747.
(57) K. Hongladarom, V.M. Ugaz, D.K. Cinader, W.R. Burghardt, J.P. Quintana, B.S. Hsiao, M.D. Dadmun, W.A. Hamilton, P.D. Butler. *Macromolecules* **1996**, *29*, 5346-5355.
(58) R.A. Segalman, H.Yokoyama, E.J. Kramer. *Advanced Materials* **2001**, *13*, 1152.
(59) T. Xu, H.C. Kim, J. DeRouchey, C. Seney, C. Levesque, P. Martin, C.M. Stafford, T.P. Russell. *Polymer* **2001**, *42*, 9091-9095.
(60) R.A. Segalman, A. Hexemer, E.J. Kramer. *Macromolecules* **2003**, *36*, 6831-6839.
(61) Segalman, R.A.; Hexemer, A.; Kramer, E.J. *Physical Review Letters* **2003**, *91*, 196101.
(62) S.M. Fontana, M.D. Dadmun, D.H. Lowndes. *In Press* **2004**.
(63) K.A. Cavicchi, T.P. Lodge. *Macromolecules* **2004**, *37*, 6004.
(64) R.A. Segalman, A. Hexemer, R.C. Hayward, E.J. Kramer. *Macromolecules* **2003**, *36*, 3272-3288.
(65) Hamley, Ian W. *The Physics of Block Copolymers*; Oxford University Press: Oxford, 1998.
(66) Fontana, S.M.; Dadmun, M.D.; Lowndes, D.H. *In Press* **2005**.
(67) Fontana, S.M.; Dadmun, M.D.; Lowndes, D.H. *In Press* **2005**.
(68) Milhaupt, J.M.; Lodge, T.P.; Smith, S.D.; Hamersky, M.W. *Macromolecules* **2001**, *34*, 5561.
(69) Birgeneau, R.J.; Kastner, M.A. *Science* **2000**, *288*, 437.
(70) Sachdev, S. *Science* **2000**, *288*, 475.
(71) Merkulov, V.I.; Melechko, A.V.; Guillorn, M.A.; Lowndes, D.H.; Simpson, M.L. *Chemical Physics Letters* **2002**, *361*, 492-498.

(72) V.I. Merkulov, D.H. Lowndes, Y.Y. Wei, G. Eres, E. Voelkl. *Applied Physics Letters* **2000**, *76*, 3555.

Vita

Scott M. Fontana was born on April 4th, 1978 in Greensburg, Pennsylvania. In 1986 he moved to Point of Rocks, Maryland where he attended grade school as well as junior and senior high school. He moved to Sevierville, Tennessee while in high school and graduated from Sevier County High School in May of 1996. In the fall of 1996 he enrolled in the University of Tennessee at Martin where he received a Bachelors of Science degree in December, 1999. He began his graduate work at the University of Tennessee at Knoxville in the fall of 2000 where he pursued a Ph.D. degree in Chemistry with a specialization in Polymer Science under the Direction of Mark Dadmun. He successfully defended his dissertation on February 11th, 2005. He accepted a position at the Food and Drug Administration in Rockville, MD beginning in February of 2005.

2034 9169 10
08/17/05 MRB